AN ARBITRARY-FUNCTION GENERATOR AND ITS APPLICATION TO THE STUDY OF SOME NON-LINEAR SYSTEMS ON THE ELECTRIC ANALOG COMPUTER

Thesis by

Werner Buchholz

In Partial Fulfillment of the Requirements
For the Degree of
Doctor of Philosophy

California Institute of Technology
Pasadena, California
1950

ACKNOWLEDGMENTS

Acknowledgments for their valuable advice and assistance are due to the members of the Analysis Laboratory, especially to Prof. G. D. McCann, under whose supervision the research was carried on, to Prof. C. H. Wilts and to B. N. Locanthi in connection with design and testing of the arbitrary - function generator, to Prof. S. Frankel in connection with theoretical questions, to Miss D. Denhard for preparing many of the drawings, and to D. H. Pickrell for some of the construction work

ABSTRACT

An arbitrary-function generator, capable of furnishing an output voltage which may be any given single-valued function of the input voltage, is described. It was constructed for use with the Electric Analog Computer at the California Institute of Technology. In principle it is an optical follower system containing a cathode-ray tube and a phototube with an opaque mask representing the desired arbitrary function.

The working model constructed is accurate to about one or two percent, has a phase shift of 3½ degrees at 2 kc and a limiting time delay of about 50 microseconds with the beam traversing a step equal to the maximum height of the function pattern employed.

Sources of error are analyzed and suggestions are made for possible improvements. A major problem which has not been solved yet satisfactorily is the local deterioration of the cathode-ray tube screen due to fatigue.

A number of non-linear problems are solved with the aid of this device, all of them dealing with second-order systems having a single degree of freedom and only one non-linear term in the equation. Among the systems discussed are series circuits with a non-linear capacitance, or mechanical systems with a non-linear spring; non-linear damping; oscillating systems, including systems behaving according to Van der Pol's equation; and mechanical systems made unstable by the presence of static (dry) friction greater than the dynamic (Coulomb) friction.

The results obtained appear to support the conclusion that the generator introduces only one or two percent of distortion, plus a small phase shift at the higher frequencies. The device makes possible the solution of many non-linear problems, hitherto inaccessible, at relatively high natural frequencies and repetition rates.

TABLE OF CONTENTS

Table of Contents - 2

INTRODUCTION

The Electric Analog Computer at the California Institute of Technology consists fundamentally of inductors, capacitors, resistors, and transformers, together with driving sources and measuring equipment. With the addition of amplifiers to provide for unilateral and active elements one can construct analogous circuits for studying systems represented by linear differential equations with constant coefficients.

To extend the range of application to a large class of non-linear systems it becomes necessary to have a device which, in its most general form, is capable of furnishing an output voltage or current which may be an arbitrary single-valued function of the input voltage. The Caltech Analog Computer operates at natural system frequencies of the order of 100 cps. and its electronic components are designed to have a phase shift of about one degree at a frequency of one kilocycle. These requirements preclude the use of mechanical linkages, and one is naturally led to look for a cathode-ray tube type of device.

Both of the arbitrary-function generators to be described in part I consist of a photomultiplier tube facing the screen of a cathode-ray tube which is partially covered by an opaque mask (usually a photographic film). Like most other electronic instruments used with the computer they are direct-coupled to avoid low-frequency instability ("motorboating") when part of a closed feedback loop.

The first type is described briefly since a considerable amount of development work was done on it before the "ancotron" idea came to the writer's attention. The latter is, however, superior in almost every respect, and the earlier device has been discarded.

The remaining sections describe some non-linear problems which were set up on the computer. The systems are all described by ordinary second-order differential equations of the type

$$\varphi_2(\ddot{x}) + \varphi_1(\dot{x}) + \varphi_0(x) = f(t) \ .$$

Only one term was made non-linear at a time. There is, of course, no fundamental difficulty in extending studies to more complex systems provided enough equipment is available.

Part II deals with systems described by

$$\ddot{x} + 2\zeta\dot{x} + x|x|^{n-1} = f(t) \ , \qquad (\zeta > 0)$$

corresponding to a mechanical system with a non-linear spring or an electrical single-loop circuit with a non-linear capacitance, and

$$\frac{1}{2\zeta}(\ddot{x} + x) + \dot{x}|\dot{x}|^{n-1} = f(t) \ , \qquad (\zeta > 0)$$

corresponding to non-linear positive damping.

No practical examples could be found where the $\varphi_2(\ddot{x})$ term is non-linear. Iron-core coils do not fall into this category since their voltage drop is given by $\frac{d}{dt}\left[\varphi(\dot{x})\right]$. As the characteristics of iron cores vary widely and no means were found for representing the all-important hysteresis properties on the function generator, it would seem more profitable to use an actual coil as its own analog.

Part III is an extension of part II to negative non-linear damping so as to cover some self-oscillating systems. In particular, Van der Pol's equation

$$\ddot{x} - \mu(1 - x^2)\dot{x} + x = 0$$

is considered as well as some other types of oscillators.

In part IV the effect of combined static friction ("stiction") and dynamic (or Coulomb) friction on an otherwise linear system is studied. Strictly speaking,

the friction force is a multi-valued function at the origin ($\dot{x} = 0$) but it is here approximated by a single-valued analytic function.

A simple thyratron circuit is shown which can replace the arbitrary-function generator in the idealized system studied.

As only single-degree-of-freedom systems are dealt with, the device is used here exclusively as a two-terminal self-impedance.

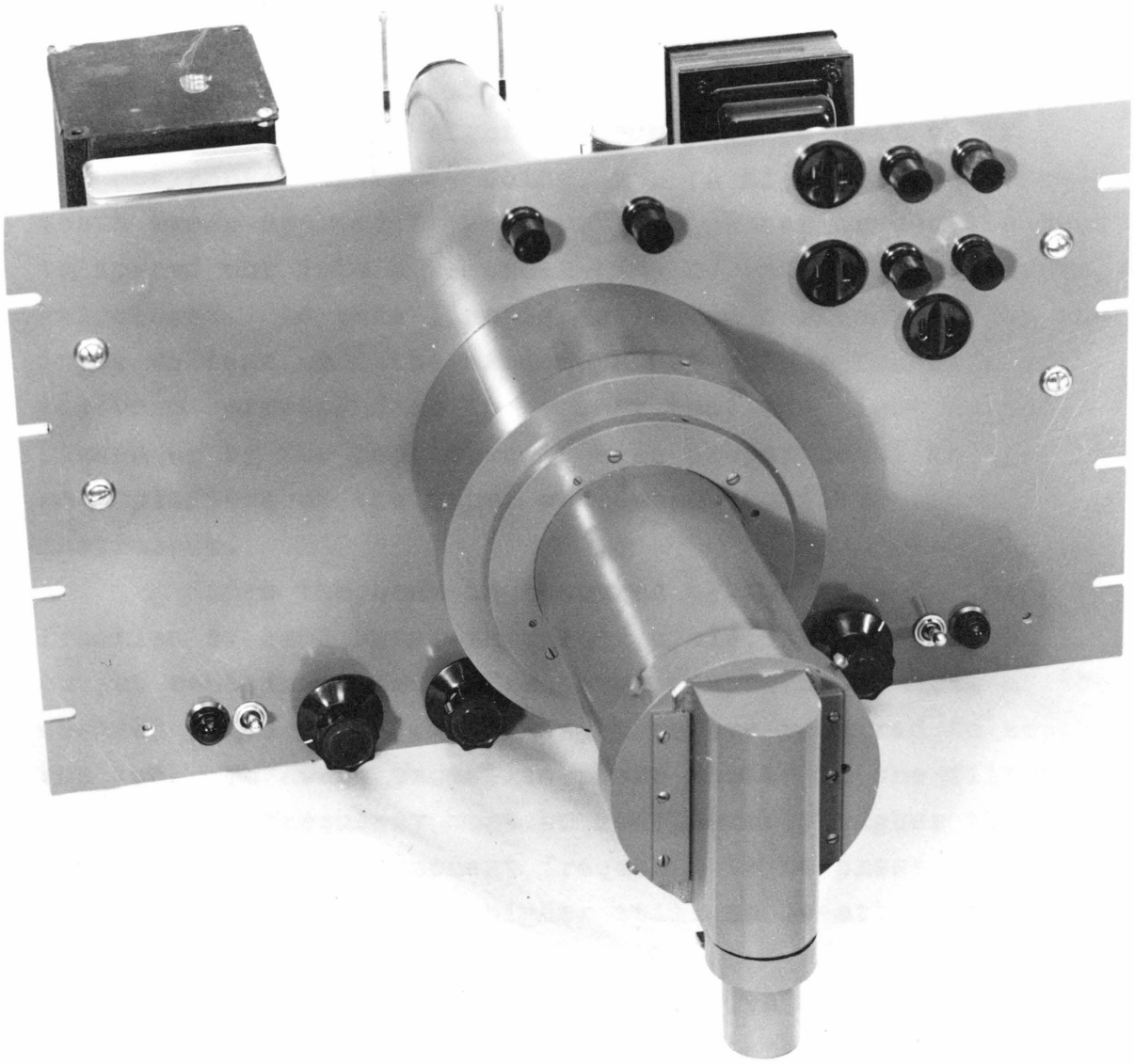

I THE ARBITRARY-FUNCTION GENERATOR

1. The Earlier Model

The function $y = f(x)$ is represented by a transparent window in an otherwise opaque mask (see Fig. 1.1). The vertical height is made proportional to y, the horizontal distance being x. A high-frequency saw-tooth sweep applied to the vertical plates causes the beam to spread out into a vertical line of essentially uniform brightness. As this line is deflected horizontally by the input voltage x, the window passes only a fraction of the beam corresponding to y, so that the light output picked up by the phototube is also proportional to y. Dc amplifiers at the input and output complete the instrument.

Since the beam is obscured by the mask during a fraction of each sweep-frequency cycle, the phototube output contains a sweep-frequency component as well as the desired voltage. A filter is therefore required to separate the two. To avoid excessive phase shifts in the filter, the cut-off frequency must be considerably higher than the highest harmonic component frequency to be passed. The sweep frequency must be higher still to be attenuated sufficiently.

A 400 kc sweep was found to give fairly good performance. At high frequencies it becomes increasingly difficult to obtain a linear saw-tooth.

This device has several obvious disadvantages. Non-uniformity in the light output of the screen, aggravated by uneven exposure of the surface to the beam during use, will cause distortion. The output voltage is low and has to be amplified. Photomultiplier tubes reduce the amplification problem but produce considerable noise. Both phototube and cathode-ray tube contribute a major part

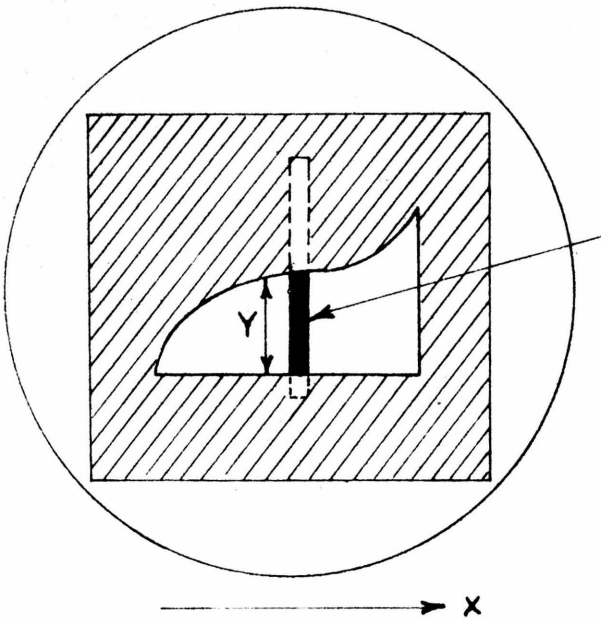

Vertical line produced by high-freq. sweep on vertical plates.

Line deflected horizontally by input voltage ~ x.

Fig. 1.1 MASK ARRANGEMENT, EARLIER MODEL OF ARBITRARY FUNCTION GENERATOR

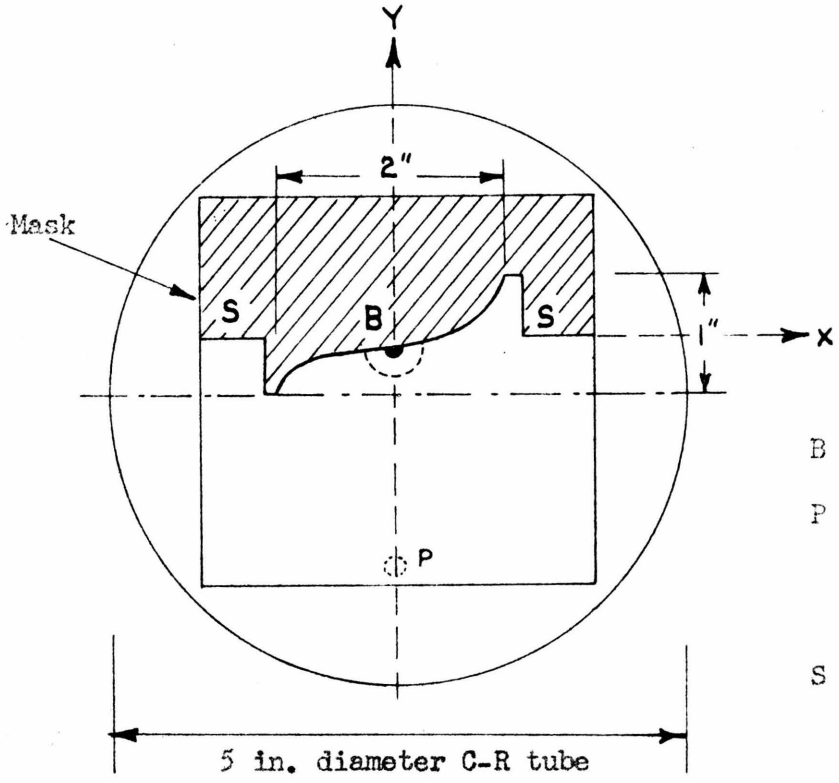

B - Beam

P - 'Off' position of beam with feedback loop open

S - Shoulders at y = 0 level

Fig. 1.2 MASK ARRANGEMENT OF ANCOTRON

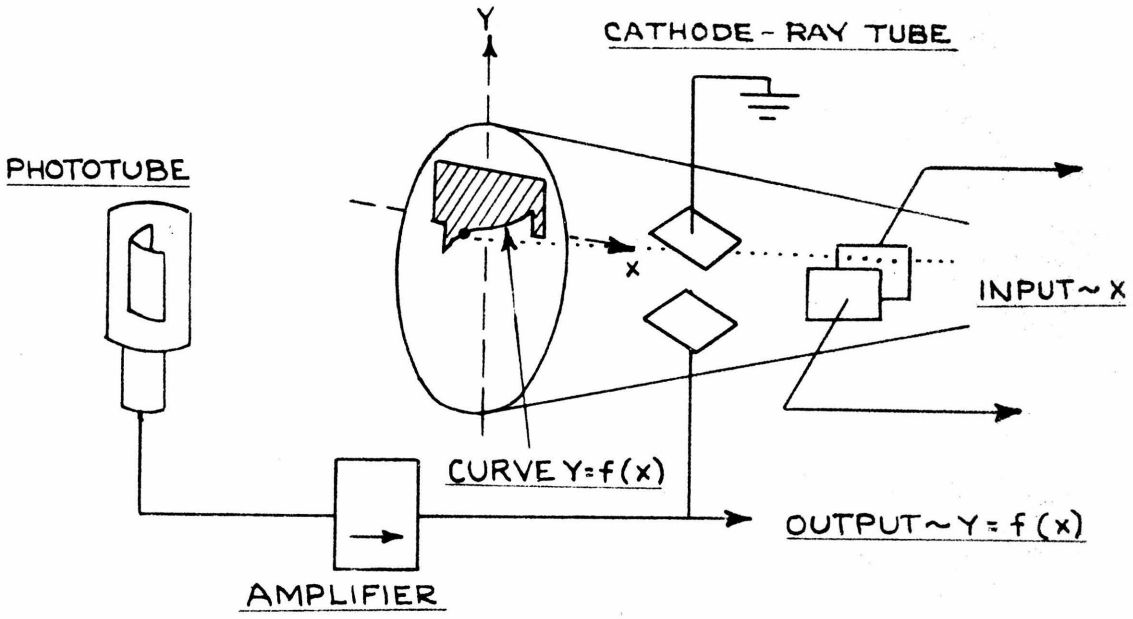

FIG. 1.3 SCHEMATIC DIAGRAM OF ANCOTRON

of the overall distortion and drift in the device.

A model was constructed which proved to be reasonably successful, nevertheless. A few simple tests were run, but no quantitative data were taken since many improvements were planned for a second version. For further details on this type of function generator the reader is referred to an article which appeared since this work was done.[1]

2. The Ancotron

The instrument to be described, which will be called an "ancotron" *, appears to have been invented in England independently by D. M. MacKay[2] and D. J. Mynall[3,4]. It is simply an optical servomechanism in which the function $y = f(x)$ is now represented by the edge of an opaque mask (Fig. 1.2).

Fig. 1.3 shows an overall schematic diagram of the ancotron. With the feedback loop open the beam of the cathode-ray tube would rest near the bottom edge of the screen. The light falls on the phototube whose output is amplified and connected to the vertical plates of the cathode-ray tube. The polarity is chosen so that the light output drives the beam upwards. Given sufficient gain in the system, the beam will come to an equilibrium at the edge of the mask. The spot is partially obscured by the mask with just enough area "visible" to the phototube so that the voltage applied to the deflection plates will keep the spot in that position.

---

* The word "ancotron" is derived from the Greek "ancōn" (ἀγκών), meaning curve (the English word anchor is derived from it), plus the ubiquitous "-tron" ending presumably obtained by splitting an "electron".

If now a voltage corresponding to x is used to move the beam horizontally, the beam is constrained to follow the edge of the pattern, so that the vertical deflection is always proportional to y. Since the voltage at the deflection plates is proportional to the deflection itself, this voltage is the desired function of the input voltage.

Fig. 1.4 shows a simplified circuit diagram of the ancotron; a complete circuit is included in appendix F for reference. A photograph of the working model appears on page 4.

Due to the feedback loop the output of the ancotron is relatively independent of the properties of the cathode-ray tube screen and the phototube. Non-uniformity of light output, noise and distortion from the phototube and from amplifier circuits inside the loop are materially reduced. A major advantage of this scheme, apart from its simplicity, is that the output voltage is the large voltage at the deflection plates. Little or no amplification is needed at the output so that full use can be made of the low-drift, low-distortion feedback loop voltage.

3. Halo

As in any servo system the spot cannot follow the mask exactly. The larger the deflection, the greater must be the area of the spot which is exposed to the phototube to provide the additional deflection voltage required. Since the spot is approximately circular the light output is not a linear function of the distance through which the spot has moved away from the pattern. For a small spot diameter the difference would be small, were it not for the "halo" surrounding the central spot.

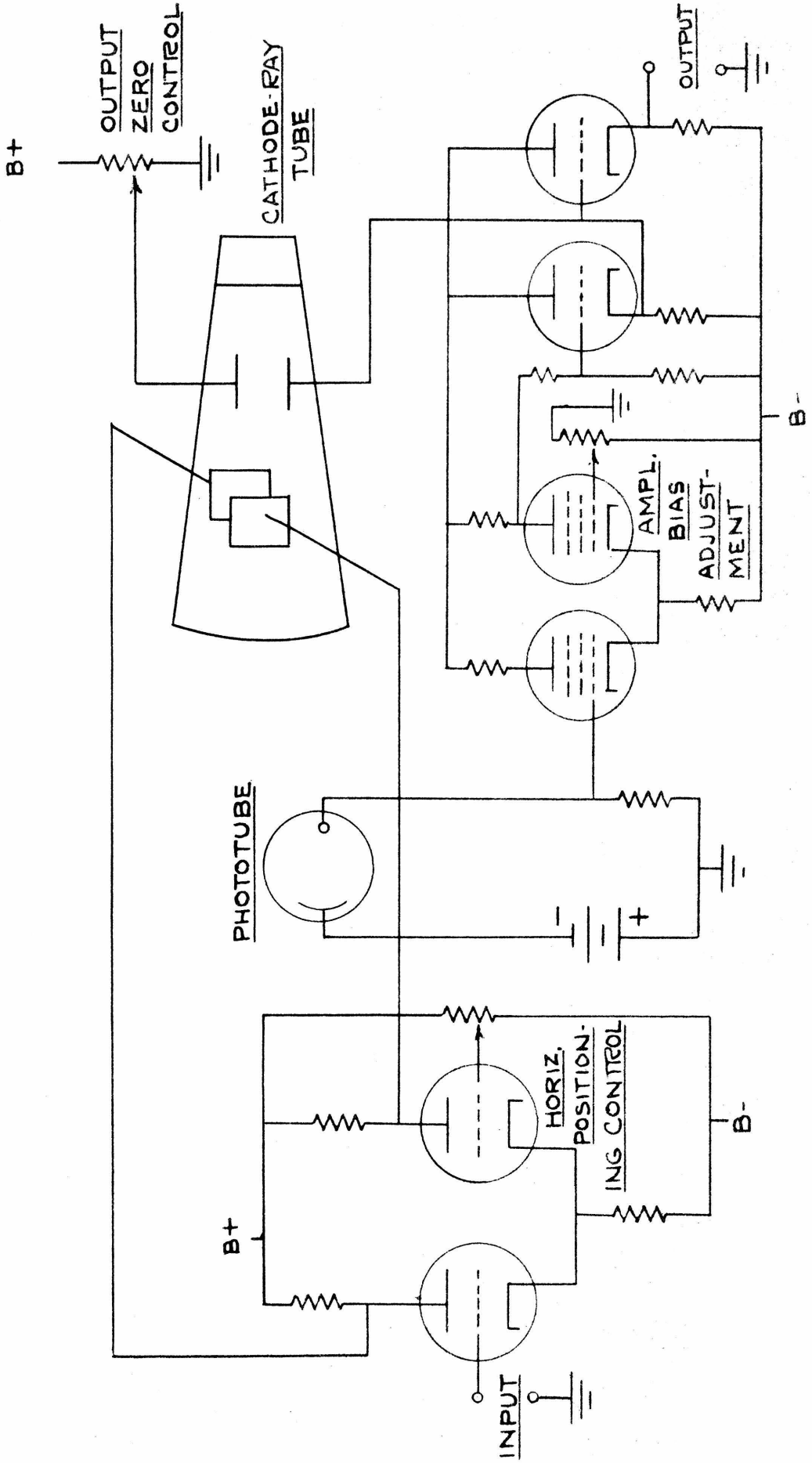

FIG. 1.4 SIMPLIFIED CIRCUIT DIAGRAM OF ANCOTRON

The halo is due to reflections inside the glass wall at the boundaries between the glass and the air or vacuum.[6] These reflections cause a set of concentric illuminated rings of decreasing brightness to appear around the central spot. The two most intense rings are indicated in Fig. 1.5 with dimensions obtained from a DuMont 5LP tube. The dimensions are a function of glass thickness and curvature.

Although the halo is hardly visible when a cathode-ray tube is operated at ordinary intensities, due to the large area and low brightness relative to the central beam, the total light emitted from the halo area is a considerable fraction of the light emitted by the spot alone. In fact, if the loop gain is made too high, the light from the bottom part of the halo alone may be sufficient to give equilibrium so that the center of the beam may be 1/8 inch or so away from the edge, behind the pattern. For a total pattern height of one inch this is a large error.

If the light output u is measured as a function of the distance ε of the center of the beam from the edge of the pattern, a curve is obtained similar to that shown in Fig. 1.6. If we assume the opaque edge to be straight near the point considered, exactly half the maximum light output U of the beam will fall on the phototube when the center of the beam is right at the edge $(\varepsilon = 0)$.

For purposes of analysis this curve will be replaced by a straight line with a slope equal to that of the curve at $\varepsilon = 0$, and extending from $\varepsilon = -h/2$ at $u = 0$ to $\varepsilon = +h/2$ at $u = U$. This is equivalent to assuming the beam to be a rectangle of uniform brightness of height h. The equation of the straight line is

$$\frac{u}{U} = \frac{1}{h}\left(\varepsilon + \frac{h}{2}\right) \qquad (1\text{-}1)$$

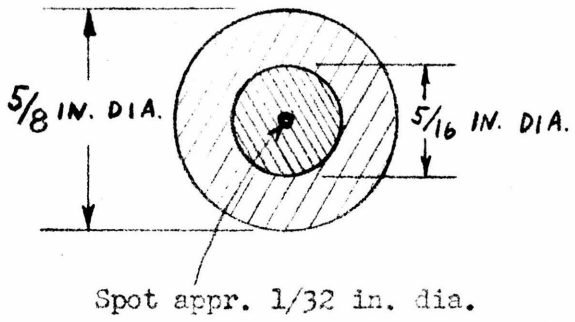

Fig. 1.5 BEAM WITH HALO RINGS

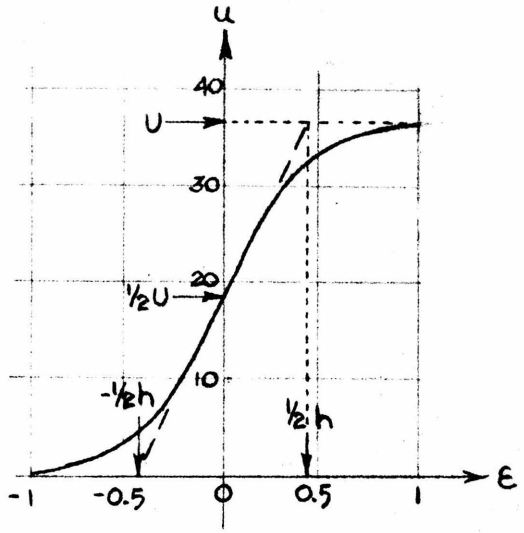

Fig. 1.6 LIGHT OUTPUT u (in terms of phototube current in μa) VS. DISTANCE ε OF BEAM FROM PATTERN EDGE (in terms of deflection voltage in volts)

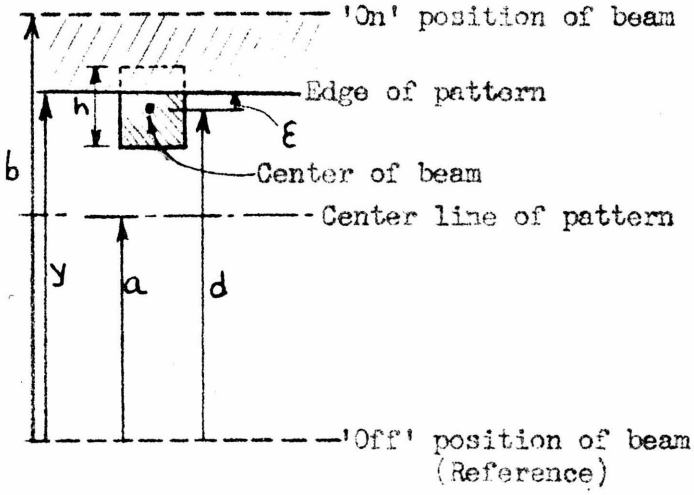

Fig. 1.7 DIMENSIONS USED FOR ANALYSIS ASSUMING RECTANGULAR SPOT

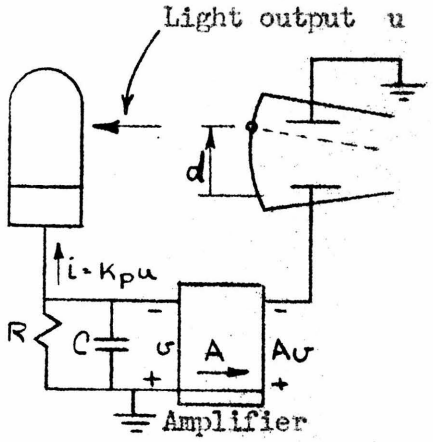

Fig. 1.8 SIMPLIFIED CIRCUIT USED FOR ANALYSIS

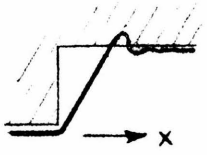

Fig. 1.9 STEP IN PATTERN

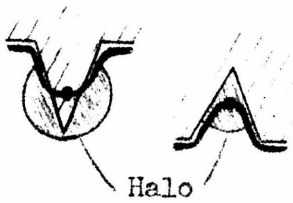

Fig. 1.10 BEAM CUTTING SHARP CORNERS

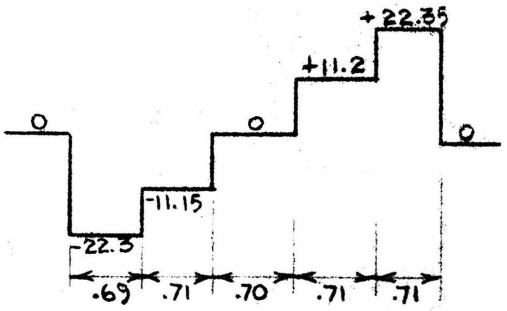

Fig. 1.11 LINEARITY TEST

4. Analysis of Ancotron Operation

For simplicity the pattern is supposed to be a horizontal straight line in the vicinity of the beam. The system is assumed to be linear over the entire range of the variables.

Referring to Fig. 1.7, let

d = actual deflection of center of beam above the reference position (where the beam is cut off),

y = height of pattern above the reference position,

$\varepsilon = y - d$ = error in following the pattern,

h = equivalent height of beam when the actual spot is replaced by an equivalent rectangle of uniform brightness and light output equal to that of the entire beam (including halo),

u = light falling on phototube for a given value of ε ,

U = maximum light falling on phototube, with entire beam exposed,

a = distance, above reference, of center line of pattern,

b = distance, above reference, of "on" position of beam (where beam is fully exposed, i.e. $u = U$).

For the circuit part of the feedback loop (Fig. 1.8), let

R = phototube load resistor,

C = stray capacitance of phototube,

A = gain of amplifier (assumed to have negligible phase shift),

K_P = phototube sensitivity (current per unit incident light),

K_D = cathode-ray tube sensitivity (deflection per volt),

$T_P = RC$ = phototube time constant,

T_D = time constant of light decay on cathode-ray tube screen (average value),

s = variable of Laplace transformation.

In terms of the Laplace transforms of the variables[7] the following equations apply:

Phototube current:

$$i(s) = K_P.u(s) \qquad (1\text{-}2)$$

Voltage input to amplifier:

$$v(s) = \frac{1}{1 + T_P s}\, i(s) \qquad (1\text{-}3)$$

Deflection:

$$d(s) = K_D A.v(s) = \frac{K_D A R K_P}{1 + T_P s}\, u(s) \qquad (1\text{-}4)$$

In the steady state the light output u will be assumed to be related to the error ε by equation (1-1). Hence the Laplace transform of u when a function of time may be written as

$$u(s) = \frac{1}{1 + T_D s}\, \frac{U}{h} \left[\varepsilon(s) + \frac{h}{2s}\right] \qquad (1\text{-}5)$$

The factor $1/(1 + T_D s)$ represents approximately the time delay due to the cathode-ray tube screen when the spot is moved, that is ε is changed suddenly. This is actually an oversimplification, but the error is a second-order effect.

Putting $d = y - \varepsilon$, the equations may be solved for ε. The factor $K_D A R K_P U$ evidently equals the total distance b through which the beam is deflected as the light output is changed from $u = 0$ to $u = U$. Thus

$$\varepsilon(s) = \frac{(1 + T_P s)(1 + T_D s).y(s) - \frac{b}{2s}}{(1 + T_P s)(1 + T_D s) + \frac{b}{h}} \qquad (1\text{-}6)$$

5. Steady-State Error and Loop Gain

Suppose the beam is suddenly deflected horizontally to a new point where $y = y_1$. This can conveniently be represented by a sudden vertical shift in the pattern at the original horizontal position. Therefore one can simply put $y(s) = y_1/s$.

The steady-state error is given by

$$\varepsilon_{ss} = \lim_{s \to 0} \left[s . \varepsilon(s) \right] \quad \text{or}$$

$$\varepsilon_{ss} = \frac{y_1 - \frac{b}{2}}{1 + \frac{b}{h}} \tag{1-7}$$

It is desirable to adjust the instrument so that the error vanishes at the center of the pattern, where $y_1 = a$. The condition to be satisfied is

$$a = \frac{b}{2} \tag{1-8}$$

Then for any position y , and since $b \gg h$,

$$\varepsilon_{ss} = \frac{h}{b} (y - a) \tag{1-9}$$

The error is thus proportional to $y - a$, the distance from the center of the pattern. This means that the total height of the pattern must be limited to a value for which the error is not excessive.

Also, to keep down the error, the factor b/h should be large. It is seen that b/h plays the role of the "$\mu\beta$" factor of feedback amplifier theory. This loop gain b/h includes, as adjustable factors, the amplifier gain A , the phototube load resistance R , the beam intensity U , and the effective spot size h . The practical considerations which limit the magnitude of these factors will be considered below.

6. Beam Position with Feedback Loop Open

One such consideration is the fact that the beam should not go off the screen and become "invisible" to the phototube when the light is interrupted, or else the feedback loop will remain open. Of course, one could manually change the circuit condition each time to bring back the beam. Some British experimenters seem to be using a manual reset button which allows a pilot light to shine on the phototube to replace the missing beam.

This is an interesting but not very satisfactory solution. The system tends to be unstable, for there are two equilibrium points, one on the edge of the pattern and one off the screen; a transient which momentarily drives the beam too far above the edge of the pattern could easily disrupt the solution if the beam decided to return to the wrong equilibrium position.

Hence the "off" position of the beam should be near but above the bottom edge of the "visible" part of the screen. This requirement is not incompatible with a high gain in the vicinity of the pattern. It is only necessary to design the amplifier to cut off at a suitable point near the bottom or to put a diode voltage limiter in the circuit.

7. Time Delays

Only two time constants, T_D and T_P, were included in the analysis since it was found that the phase shifts in the rest of the circuit could be kept small in comparison. To reduce T_D the cathode-ray tube should have a short-persistence phosphor. The best available phosphor is the P 15 which is a zinc-oxide coating with a decay time around one microsecond when used without a filter. The light output is of a bluish green color.

The P 5 phosphor has a decay time closer to ten microseconds and a blue color of apparently less intensity than the P 15. The P 15 phosphor was found not to give sufficiently improved performance to make the (present) extra cost worth while.

The major offender is T_P due to the multiplier phototube capacitance. Its effect cannot be reduced by lowering the load resistor, for this lowers the loop gain by the same amount. The deflection $d = y - \varepsilon$ is given by

$$d(s) = \frac{y(s) + \frac{h}{2s}}{1 + \frac{h}{b} \cdot (1 + T_P s)(1 + T_D s)} \qquad (1\text{-}10)$$

For small values of s, neglecting terms in s^2,

$$d(s) \approx \frac{y(s) + \frac{h}{2s}}{(1 + \frac{h}{b})\left[1 + \frac{T_P + T_D}{1 + \frac{b}{h}} . s\right]} \qquad (1\text{-}11)$$

Thus the effective time constant is

$$T_e = \frac{T_P + T_D}{1 + \frac{b}{h}} \qquad (1\text{-}12)$$

or if $T_P \gg T_D$ and $b \gg h$,

$$T_e \approx \frac{h}{b} T_P = hK_D AK_P U.C \qquad (1\text{-}13)$$

R has canceled out. R can therefore be made large to reduce distortion, but not so large that the higher terms in s, so far neglected, enter to produce instability at very high frequencies.

It should be recognized, however, that this theory applies only as long as the system remains linear. Suppose the beam is moved past a step in the pattern, as shown in Fig. 1.9. If the velocity $\dot{x}$ is high enough the time delay may cause the beam to leave the edge entirely. The full light output U incident on the phototube causes it to charge the capacitance with a constant current $K_P U$. The voltage rises at a constant rate $K_P U/C$ giving the beam a constant vertical velocity $K_P UAK_D = b/T_P$ until it reaches the edge of the pattern again. Similarly, going the other way the beam may disappear entirely so that the velocity is given by the rate of discharge of C through R. Both times the feedback loop remains in effect open during the transition.

Thus, in contrast to linear systems, the limiting time delay depends on the size of the step, being

approximately proportional to the height. In the actual unit constructed this time delay when going across a step was found to be about 50 microseconds per inch deflection.

On the other hand, with a fairly smooth pattern, the time delay may be much less. For a gradually rising straight-line pattern (which effectively converts the ancotron into a linear amplifier) with a sinusoidal input voltage, a phase shift of $3\frac{1}{2}$ degrees was observed at a frequency of 2 kc, or a time delay of only 5 microseconds.

It was interesting to observe, on an oscilloscope set up for phase shift measurement, the effect of raising the frequency. Just above 4 kc one half of the ellipse was seen to expand rapidly to a much larger size. As the adjustment of the system was not quite symmetrical, the feedback ceased to be effective on one side when the beam was still tracking the pattern on the other side.

8. Amplifier Gain

The amplifier gain cannot be increased too far either. The addition of high-gain stages puts more $1/(1 + Ts)$ factors into the gain expression. Although each T may be small compared to $T_P + T_D$ so that the phase shift in the operating range is not increased materially, the higher-order terms become noticeable at very high frequencies, leading to parasitic oscillations.

This is a major reason also for choosing a photomultiplier rather than an ordinary phototube which does not need a high-voltage power supply; the additional stages required tend to cause instability.

A possible alternative is to construct a larger number of wide-band low-gain stages, but this was not considered worth while.

9. Beam Intensity

Finally, it is not desirable to try to secure a larger loop gain by operating at a high beam intensity. For one thing, even with proper focus, the spot size h tends to increase with the intensity U , so that the gain, which is proportional to U/h , does not increase nearly as much as does the intensity.

Moreover, a high intensity seriously limits the useful life of the phosphor due to fatigue. It is well known that continued electron bombardment of one spot on a cathode-ray tube produces "burning", a permanent discoloration of the screen material. But long before this becomes visible a drop in phototube output may be noticed when the beam is stationary.

The phosphor recovers only partially, and a permanent "dead spot" remains. If the drop in intensity is enough to reduce the feedback below the level required for adequate tracking, a "bump" is seen to develop at that spot: the beam neatly detours the area, as surely as if the "bump" were permanently inked in on the pattern.

Unfortunately, the beam cannot always be kept moving. Many problems on the computer are transient studies where the system is periodically (at a 10 cps. rate) returned to the initial conditions. Hence the beam must return to the starting point during each cycle and remain there for as much as half the period. Thus the beam may be stationary for half the total time spent on a problem, which could be many hours. Furthermore, for symmetrical patterns the point of rest is usually the center of the pattern, and if the pattern position remains fixed the effect is clearly cumulative.

The few remedies that come to mind are only partial ones. One is to keep the intensity as low as possible. But "dead spots" already in existence will be less

noticeable if the loop gain is high. The reduction in intensity must therefore be compensated for by raising the gain elsewhere. It seems also that the P 5 phosphor may be a little less susceptible to "dead spots" than the P 15 , but no conclusive data were obtained on this point.

A thorough study of the fatigue problem should be made. Perhaps a more stable phosphor can be found. The dead period for transient studies should, of course, always be kept as short as possible, and the beam should be turned off when not in use.

10. Cathode-Ray Tube Distortion

So far the cathode-ray tube has been assumed to have a constant deflection sensitivity K_D . Since the actual output is not the deflection d but the deflecting-plate voltage d/K_D , any non-linearity which makes K_D a function of the deflection will cause distortion in the output - and feedback can do nothing about it.

If "single-ended" amplification is used, where the deflecting voltage v_D is applied only to one of a pair of deflecting terminals, the other being grounded, there is an average potential between the plates of $v_D/2$ with respect to the second anode (assumed grounded as is usually the case). Let the second anode-to-cathode accelerating voltage be V_{ao} . The effective accelerating voltage is now

$$V_a = V_{ao} + \frac{v_D}{2} \qquad (1\text{-}14)$$

The deflection is[8]

$$d = G \frac{v_D}{V_a} \qquad (1\text{-}15)$$

where G is a geometric constant. Hence

$$d \approx G \frac{V_D}{V_{ao}} \left(1 - \frac{V_D}{2V_{ao}}\right) = d_o - \frac{d_o^2}{2G} \qquad (1\text{-}16)$$

where d_o is the linear deflection. The distortion thus adds a square-law term to the deflection.

By using symmetrical "push-pull" deflection such distortion could be avoided. At the vertical plates this cannot be done since the voltage must be supplied with respect to ground at the output. As there is no satisfactory way of going from "push-pull" to "single-ended" operation for dc amplifiers, the whole vertical deflection system has to be "single-ended". According to equation (1-16) the distortion for a given tube can be made smaller only by reducing the maximum deflection.

There is also an interaction between the plates giving rise to a trapezoidal distortion if one of the second pair of plates is grounded.(9) Trapezoidal distortion, as well as distortion in the horizontal deflection, can be eliminated by making the second pair (nearest the screen) the horizontal deflecting plates and supplying them from a balanced "push-pull" amplifier.

Another possible source of distortion is the post-deflection accelerating potential employed in the DuMont 5LP series tubes. If this potential is too high, compared to the potential between second anode and cathode, the sensitivity will be found to decrease towards the edge of the screen.

11. Optics

In the present model the phototube is mounted at a distance of seven inches from the cathode-ray tube inside a light-tight housing. A small hole drilled into the housing permits observing the beam; the stray light admitted through it does not disturb operation. No lens

is being used.

The interior of the housing is painted black and baffles are provided to prevent light reflected from the walls from reaching the phototube. Otherwise the amount of light received will depend considerably on the position of the beam.

For a given distance from the screen the light intercepted by the phototube from the luminescent spot on the screen varies approximately as $\cos^4\theta$, where θ is the angle between the axis and the line joining the spot and the center of the phototube. Thus the effective light output is reduced as the beam is deflected off the axis even if the beam is fully exposed. But for a 5:1 ratio of phototube distance to deflection this effect changes the loop gain by less than 10 % which is not serious.

Some parallax errors are unavoidable since screen curvature and thickness both prevent the mask from being closely adjacent to the luminescent spot. Tubes with flatter screens than the 5LP series are available but they usually have a thicker glass face. To reduce parallax to a minimum the flat film is made to follow a cylindrical surface which makes contact with the spherical cathode-ray tube face at least along the horizontal center line; also the deflection is kept to only a fraction of the available screen area.

The addition of a collecting lens which would focus the screen on to the plane of the phototube cathode would greatly increase the phototube output. This would serve to raise the loop gain without any loss in stability, an advantage which might offset mechanical complications. A large-aperture lens might also reduce optical distortions by increasing the ratio of direct to indirect (reflected) light received and by averaging out parallax and the "$\cos^4\theta$" effects over its larger area. Some experimenting would be required to establish this point.

12. Tracking Errors

There are a number of reasons arising from the above considerations why the beam may not follow the pattern accurately:

(1) On page 17 it was shown that the beam has a maximum vertical velocity of approximately b/T_p which limits the slope of the pattern that the beam can follow for a given horizontal velocity. If the horizontal deflection is a saw-tooth of magnitude X and frequency f, the horizontal velocity is Xf. Therefore the maximum slope of the pattern is $b/(XfT_p)$.

(2) If the system is not adjusted so that $a = b/2$ (equation 1-8), which causes the beam to be just half exposed at the center of the pattern, and if the system has a high gain, the beam may operate on the halo alone, giving a tracking error of the order of the radius of the halo, about 1/8 inch for the 5LP tube.

(3) If the gain is insufficient the beam may be unable to reach the higher points on the pattern. The multiplier phototube should be mounted with the cathode surface normal to the axis to avoid losing gain when the light comes from the side. This would cause "drooping" of the pattern on one side.

(4) For purposes of analysis, on page 13, it was assumed that the edge of the pattern was straight. If the curvature is large the light output may be materially altered by the fact that either more or less than half the halo area will be exposed depending on whether the pattern is convex or concave. The result is that the beam will tend to cut sharp corners as shown in Fig. 1.10. Proper adjustment, as in paragraph (2) above, will reduce the contribution of

the halo to this effect, but it is evident that the spot diameter itself gives an ultimate limit to the resolution which can be achieved.

13. Details of Construction

The cathode-ray tube being used is the 5-inch DuMont 5LP5A which has a low enough decay time and is (at present) more easily available at less cost than the 5LP15 . For similar reasons the 931A multiplier phototube was chosen over the 1P28 , even though the latter has a greater response to the blue trace of the P 5 phosphor. Moreover, the variations among different specimens of the 931A were found to be greater than the difference between the average 931A and the 1P28 (of which only one was available for test).

The horizontal amplifier is a single grounded-grid phase inverter stage. A dc voltage applied to the unused grid serves to position the beam horizontally. A reversing switch makes it possible to interchange the two grids, thus changing the sign of the output voltage without the use of an extra phase reversing amplifier. This is especially useful when the ancotron is connected to function as a two-terminal impedance; both positive and negative impedances can be simulated with the same set of input and output amplifiers.

The phototube anode is directly connected to a phase inverter type amplifier. The output is taken off only one of the plates, since as explained above the vertical amplifier must remain "single-ended". The major reason for using this construction is that cathode and screen degeneration are avoided giving a high gain good to dc. Also the extra grid provides a convenient way of inserting a dc voltage into the amplifier for adjustment.

The use of this "bias adjustment" will be explained later. The small capacitance between grid and plate of the first tube was added to stop oscillations. Unfortunately, a capacitance at this point considerably increases the effective phototube time constant T_P .

The amplifier stage is followed by two consecutive cathode followers. The first one isolates the deflecting plate and connecting lead capacitance from the amplifier. The second one isolates the output terminal from the whole feedback loop. Without it even a fairly small capacitance across the output terminals was enough to start oscillations.

To provide a means for adjusting the output voltage to zero when the beam is set to the zero level on the pattern, a variable dc bias is applied to the unused deflection plate. If this voltage is changed, the feedback loop will provide a compensating voltage on the other plate, and hence at the output also, in order to keep the beam at the edge of the pattern.

The remainder of the circuit consists of power supplies and voltage regulators. In particular, the negative supply for the photomultiplier and the cathode-ray tube is regulated at 1000 volts to reduce drift due to line voltage fluctuations. The 7F7 tube with loctal base has been found to withstand satisfactorily operation in the regulator circuit at voltages well above normal ratings.

Details of the mask are shown in Fig. 1.2. For reasons outlined the working area has been restricted. The pattern size is limited to 1 inch vertically and 2 inches horizontally. The pattern is produced by first drawing a graph of the function $y = f(x)$ on rectangular coordinate paper to four times the final scale, i.e. 4x8 inches, for greater accuracy. The graph is then copied on a white cardboard. The curve is carefully inked with a

fine pen. Shoulders are added along the $y = 0$ line to facilitate zeroing the output; these are indicated by the letter S in Fig. 1.2. The part above the curve is filled in with India ink.

The pattern is then photographed, reduced in size 4:1, on high-contrast low-shrinkage litho film. From the negative a contact print is made, again on litho film. Both films are exposed and developed for maximum contrast. The positive is finally reduced with Farmer's reducer until the light area is completely clear, as clear as unexposed film. This avoids unnecessary loss in intensity and loop gain. It does not matter if the dark area loses some density in the process so long as the contrast is still high.

It is possible to compensate for any remaining distortion, which is a function of the deflecting voltages only, by pre-distorting the pattern. This scheme has been abandoned not only because of the added complications in preparing a pattern but also because the pre-distortion is a function of the pattern position. It would seem desirable to be able to shift the patterns slightly on the cathode-ray tube screen, in case "dead spots" have developed in the former position after prolonged use. But then the pattern corrections would have to be changed too, and old patterns could not be used again without losing accuracy.

It is thought that the present model already has an acceptably low level of distortion, and any further reductions would be better made at the source of distortion.

The finished pattern must be accurately positioned so that its coordinate axes are parallel to those of the cathode-ray tube. This is done by rotating the mask holder and phototube assembly and then clamping it into position with set screws. Vertical and horizontal positioning is done electrically, however, as described.

14. Adjustment of Ancotron

(1) Insert a pattern. Set the intensity to a reasonable value and focus.

(2) Move the spot with the horizontal positioning control to a point on the pattern which is halfway between the vertical extremes.

(3) Set the "bias adjustment" until the plates of the phase inverter (V_1, V_2) are at the same potential. (This ensures that the amplifier is balanced and has maximum gain in the region of the pattern.)

(4) Use the "output zero" control to bring the output voltage to zero.

(5) Ground the input grid (or remove the phototube) and check whether the beam is still "visible" to the phototube. If not, the intensity may have to be reduced.

Repeat (3), (4), and (5) until conditions are met simultaneously.

(6) With the beam still in the position it had in paragraph (2), measure the phototube output voltage with a dc vacuum-tube voltmeter (a test jack is provided on the panel).

(7) Remove the vertical-amplifier tubes (V_1, V_2, V_3) from their sockets and short the two vertical deflection plates together. Remove the pattern. Thus, with the beam fully exposed, measure the phototube output voltage again. This voltage should read approximately twice the value found in paragraph (6) to satisfy equation (1-8).

If the voltage in (7) is found to be considerably high or low this means that the design is not such that optimum performance can be realized. It may still be possible to change the intensity and bias adjustments to obtain an acceptable compromise such that the beam will

follow the pattern with sufficient accuracy. Care should be taken, however, that the phase inverter is not unbalanced so far that one of the tubes is cut off.

After the above set of adjustments has been found to give satisfactory operation it should not be necessary to touch the intensity, focus, and bias controls unless tubes have to be replaced. Ageing of tubes and the cathode-ray tube screen may require an occasional trimming of the controls. Otherwise for normal operation the following procedure will suffice:

(8) Move the spot to one of the shoulders S (see Fig. 1.2) and adjust the output to zero. Move to the other shoulder. If the output is no longer zero the pattern has to be rotated. The pattern is positioned properly when the output reads zero on both shoulders of the pattern.

(9) Move the beam to the $x = 0$ position and adjust the output to the proper voltage corresponding to $x = 0$.

Note: The beam should always be turned off when not in use. However, this results in a large dc voltage at the output terminals so that other equipment should be protected. Also to avoid overloading the multiplier phototube with stray light, the set should be turned off before taking the assembly apart to change patterns, etc.

15. Use and Calibration

In many applications the input voltage available may not be large enough to drive the ancotron. In such cases an external input amplifier is required. Also the output circuit was not designed to provide power at low impedance, and an output amplifier may have to be added.

For reasons of simplicity and flexibility such amplifiers were not incorporated into the present instrument.

As it stands, the ancotron is a three-terminal device. Since the two pairs of deflection plates are independent, provided the average potential of each pair with respect to the second anode is not too high, it is quite possible to separate the input and output circuits electrically and make a four-terminal device out of it. This requires separate power supplies and well-shielded power transformers. But the impedance between the circuits would have to be kept low to avoid instability.

A non-linear device is somewhat more difficult to calibrate than a linear one. It is necessary to know both input and output voltage at a particular value of the transfer function. The problem is simplified by using dimensionless variables.

Instead of $y = f(x)$ the function is better written

$$y = y_0 \cdot \varphi\left(\frac{x}{x_0}\right) \qquad (1\text{-}17)$$

where $y = y_0$ when $x = x_0$, i.e. $\varphi(1) = 1$. $\varphi(x/x_0)$ represents the non-linearity as a dimensionless normalized function. The set of specific values (x_0, y_0) then determines the numerical level and the dimensions for a particular problem. (x_0, y_0) may be any characteristic point, such as the extreme point beyond which the function ceases to apply, or an asymptotic point, or a stationary value along the curve. But any other point will also do since $\varphi(x/x_0)$ is assumed to be single-valued.

Thus for calibration it is only necessary to apply a voltage corresponding to x_0 and to measure the output voltage y_0. For accuracy they should be near the extreme of the pattern.

To make the results obtained general, they should always be expressed in terms of dimensionless variables,

such as x/x_o and y/y_o. When applying the results to predict the performance of an actual system the point (x_o, y_o) will be chosen to fit that system. The dimensions of x and y and the numerical magnitudes may be entirely different from those of the analog.

16. Performance

To test the linearity of the device a step pattern of accurate dimensions was used. Each step was 1/4 inch in height and width. In fig. 1.11 the corresponding output voltages are shown at each step. Underneath are given the input voltages required to go from one step to the next. All readings were taken with dc meters.

The output voltage is seen to be proportional to the pattern height with an error of considerably less than 1 % . The horizontal deflection shows a somewhat larger departure from linearity, but the error is also less than 1 % .

As already mentioned, the phase shift with a straight-line pattern of slope = $\frac{1}{2}$ and sinusoidal input was $3\frac{1}{2}$ degrees at a frequency of 2 kc. For very steep slopes the limiting time of rise is about 50 microseconds per inch of vertical deflection.

The drift is tolerable but still large enough to require frequent resetting. The major offender appears to be the horizontal positioning voltage.

Further conclusions about accuracy can be drawn from the examples discussed in succeeding sections. It appeared that the errors which occurred were due more to the recording equipment used than to the ancotron. Lack of time prevented any attempt to improve the calibration methods.

17. Suggestions for Improvements

The present version of the ancotron was intended only as a working model, and no attempt was made to perfect the mechanical design, especially of the mask holder which is of a rather primitive nature.

Since no voltage limiter is incorporated in the present circuit to keep the beam from leaving the screen, this design is limited in the maximum loop gain that can be used without obtaining tracking errors due to halo. If a simple diode limiter were added it would be feasible to raise the gain considerably by adding a lens or changing the circuit, provided oscillations can be avoided. If the additional gain is not required to improve accuracy, the intensity could be reduced correspondingly to avoid "dead spots" and increase tube life.

The VR tubes should be replaced by a vacuum-tube regulator with a battery to reduce drift. A beam switch or relay which would turn off the beam and at the same time insert a dc voltage to replace the phototube voltage would simplify operation by avoiding the large dc voltage output which otherwise occurs when the beam is turned off.

A means for setting the beam horizontally to a predetermined position by eye would simplify the zeroing problem. A mark on the pattern itself is not visible in the dark. But a mechanical pointer placed in front of the pattern from above at the desired horizontal position would force the beam to travel around the tip of the pointer. After the beam has been positioned at the tip, the pointer is withdrawn upwards to remove it from the path of the beam.

II SOME NON-LINEAR SYSTEMS WITH ONE DEGREE OF FREEDOM

1. Introduction. Linear Systems with One Degree of Freedom

Consider as an example a single-loop electrical R-L-C circuit. In terms of the charge q, capacitance C, resistance R, inductance L, and driving voltage e, the differential equation is

$$e = L\ddot{q} + R\dot{q} + \frac{q}{C} \qquad (2\text{-}1)$$

where the dots denote differentiation with respect to the time t.

Let $e = E f(t)$, where E is a characteristic value of the voltage e (such as the maximum) and $f(t)$ is a dimensionless function of time. Also let $x = q/(CE)$, a dimensionless variable. Then the equation becomes

$$f(t) = LC\ddot{x} + RC\dot{x} + x \qquad (2\text{-}2)$$

Let $\omega_o = 1/\sqrt{LC}$, the natural frequency of oscillation and $\alpha = R/(2L)$, the damping coefficient. Also we shall introduce a dimensionless time variable $\tau = \omega_o t$. Since $\dot{x} = \omega_o \cdot dx/d\tau$, etc., we now have

$$f(\tau) = \frac{d^2x}{d\tau^2} + 2\zeta\frac{dx}{d\tau} + x \qquad (2\text{-}3)$$

where $\zeta = \frac{\alpha}{\omega_o}$, the relative damping coefficient, a dimensionless parameter.

All other linear single-degree-of-freedom systems, whether of electrical, mechanical, or other nature, can be reduced to this differential equation in terms of dimensionless variables and the single parameter ζ.

In terms of the parameter $Q = \frac{\omega_o L}{R} = \frac{1}{\omega_o CR}$ frequently used for series resonant circuits (L, R, C in

series) or its equivalent value $Q = \frac{R}{\omega_o L} = \omega_o CR$ for parallel resonant circuits (L, R, C in parallel) the parameter is given by $\zeta = \frac{1}{2Q}$.

The simplest transient forcing function that can be applied is the unit step:

$$f(\tau) = \begin{cases} 0 & \text{for } \tau < 0 \\ 1 & \text{for } \tau > 0 \end{cases} \qquad (2\text{-}4)$$

It is well known that
for $\zeta < 1$ the system will be oscillatory (underdamped),
for $\zeta > 1$ the system will be overdamped, and
for $\zeta = 1$ the system will be critically damped.

For non-linear systems critical damping will occur at different values of ζ . The critical value will be called ζ_c .

An easily measured indication of the "time of rise" in the critically damped case is the time at which $x = \frac{1}{2}$. In terms of dimensionless "time" this will be called τ_c and it can be shown (appendix A) that for a linear system

$$\tau_c = 1.68 \qquad (2\text{-}5)$$

Many practical systems are designed to be slightly underdamped to obtain a faster response at the expense of some overshoot. As a typical example the condition for 10 % overshoot was found (appendix B). For the linear case the value of ζ turns out to be

$$\zeta_{10} = 0.591 \qquad (2\text{-}6)$$

and the time at which the first maximum occurs is

$$\tau_{10} = 3.90 \qquad (2\text{-}7)$$

Similar values will be obtained for the systems with non-linear capacitance.

For a steady-state sinusoidal forcing function of angular frequency ω ,

$$f(\tau) = \sin \frac{\omega}{\omega_o} \tau \qquad (2\text{-}8)$$

In the linear case resonance occurs at $\frac{\omega}{\omega_o} = 1$.

2. Non-linear Elements

Non-linear elements may be characterized by the fact that the corresponding parameter in the differential equation is not constant. If we restrict our discussion to parameters which are a function of a dependent variable only, this means that for a non-linear capacitance, for instance, $C = C(q)$. Hence the voltage across the capacitance is $v = \frac{q}{C(q)}$.

This commonly used method of describing the non-linear element is, however, highly artificial. It requires the multiplication or division of two functions of the same variable, here q and $C(q)$. This extra step may not be of much consequence in numerical work, although nothing is gained by it.* But it is a needless complication in setting up an analog circuit.

Instead we shall always use the function $v = v(q)$ as describing a non-linear capacitance, etc., and variable parameters will be avoided in the discussion. The terms "capacitance","resistance", etc., will be retained, however, to describe the general character of the impedance element. In general, then, the voltage across a capacitance is $v = v(q)$, across a resistance $v = v(\dot{q})$, and so on.

3. Types of Non-linear Elements Considered

In order to choose some particular cases from the

---

*We have excluded here such cases as $C = C(t)$ which occur, for instance, in reactance tube circuits. There the parameter notation is justified.

infinite number of theoretically possible functions it was decided to consider functions of the form

$$y = \pm |x|^n$$

where n may be any positive number, not necessarily integral, and the sign is that of x. The function can be written more explicitly

$$y = x|x|^{n-1}, \quad n > 0 . \qquad (2\text{-}9)$$

y is an odd function of x, i.e. it is symmetrical about the origin. See Fig. 2.1.

Many non-linear elements encountered in practice can be approximated by such a function if the value of n is chosen properly. It is only necessary to plot experimentally obtained curves on log-log graph paper and to find the average slope of the line.

Examples for which $n < 1$ are elements which tend to saturate, such as the plate resistance of pentode tubes. Into the class for which $n > 1$ belong springs with increasing stiffness, damping which increases with velocity, etc. Only near the origin does the approximation break down since there the slope becomes infinite ($n < 1$) or zero ($n > 1$); but this is not serious if the amplitude is large and the variables do not remain near the origin for an appreciable length of time.

Another reason for making this choice is that some results may be checked analytically without much difficulty.

4. Representation of Non-linear Two-Terminal Impedances

The circuit used is shown in Fig. 2.2, where the diamond-shaped symbol represents the ancotron plus input and output amplifiers. The voltage across the element, V, is made up of the output of the ancotron plus the voltage drop v across the linear reference impedance Z.

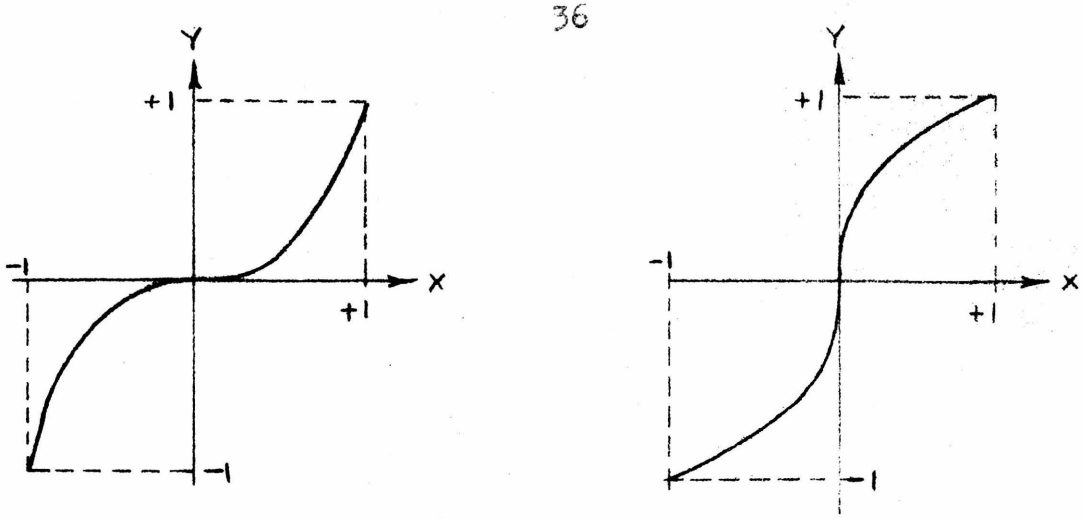

(a) $n>1$ (b) $n<1$

Fig. 2.1 EXAMPLES OF NON-LINEAR FUNCTIONS OF TYPE

$$y = x.|x|^{n-1}, \quad n>0$$

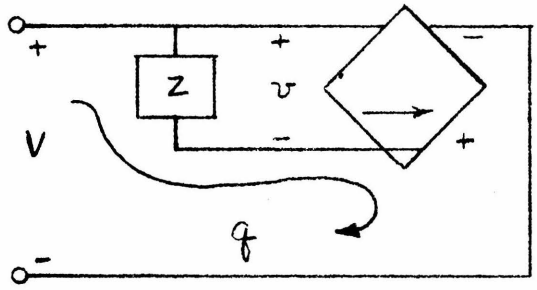

Fig. 2.2 GENERAL CIRCUIT USED FOR NON-LINEAR IMPEDANCE

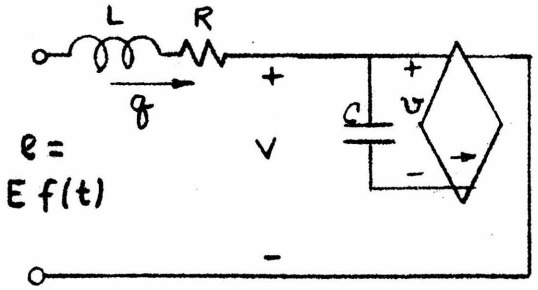

Fig. 2.3 CIRCUIT FOR NON-LINEAR CAPACITANCE

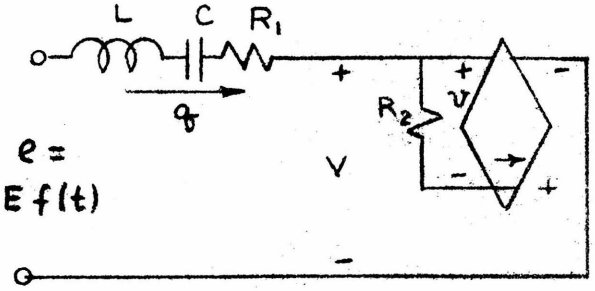

Fig. 2.4 CIRCUIT FOR NON-LINEAR RESISTANCE

The output impedance of the amplifier used was low enough to be negligible. But the linear term v has to be compensated for.

This can be done by producing a pattern according to the function

$$y = x\,(1.1\,|x|^{n-1} - 0.1) \qquad (2\text{-}10)$$

between the limits $-1 \leqslant x \leqslant +1$, instead of equation (2-9). Then the linear term will cancel if the gains are adjusted so that at the extremes of the pattern ($x = 1$) the output voltage is exactly ten times the input voltage, that is, $V_{max} = 11.0\ v_{max}$.

As an alternative to this procedure the gain can be made so large that $V \gg v$, provided the high gain does not lead to parasitic oscillations.

5. System with Non-Linear Capacitance

The equations for the system of fig. 2.3 may be derived as follows.

$$e = E\,f(t) = L\,\ddot{q} + R\,\dot{q} + V \qquad (2\text{-}11)$$

Let $v = \frac{q}{C}$

$x = \frac{v}{v_o}$

$V = V_o\,\varphi(x)$

and $K = \frac{V_o}{v_o}$

where $v = v_o$ when $V = V_o$. V_o may be any reference voltage (see discussion on page 29), but it is convenient to make $V_o = E$. Then the equation becomes

$$f(t) = L\,\frac{C}{K}\,\ddot{x} + R\,\frac{C}{K}\,\dot{x} + \varphi(x) \qquad (2\text{-}12)$$

Now let $\omega_o = 1/\sqrt{LC/K}$ and $\tau = \omega_o t$. Then

$$f(\tau) = \frac{d^2x}{d\tau^2} + 2\zeta\frac{dx}{d\tau} + \varphi(x) \qquad (2\text{-}13)$$

where $\zeta = \frac{R}{2}\sqrt{\frac{C}{LK}}$, the relative damping coefficient.

The parameter ζ and the form of the function $\varphi(x)$ completely define the system. Note that $\varphi(1) = 1$ by definition.

The actual functions used were

$$\varphi(x) = x|x|^{n-1} \qquad (2\text{-}14)$$

with values for n of $\frac{1}{3}$, $\frac{1}{2}$, 2 , and 3 .

Fig. 2.5 shows the complete circuit for representing systems with a non-linear capacitance and a constant voltage suddenly applied. The switches S_1 and S_2 are relays which are opened and closed in synchronism at a rate of 10 cps. S_1 applies the voltage to the circuit and S_2 discharges the condenser during the off-period to re-establish the initial conditions. Most of the transient studies are thus actually of the form of repeated transients to facilitate observation on and recording from an oscilloscope. However, single transients obtained by manual switching can also be used. The purpose of R_o is to allow the current to die out during the off-period without arcing at the switch contacts; it does not interfere during the on-period since it is in parallel with a low-impedance source.

6. Results for A Unit Step Suddenly Applied

The conditions for critical damping and for 10 % overshoot were obtained experimentally for each n . Values of ζ_c, τ_c, ζ_{10}, and τ_{10}, as described on page 33 for the linear case, were calculated from the known circuit parameters and the time measurements which were

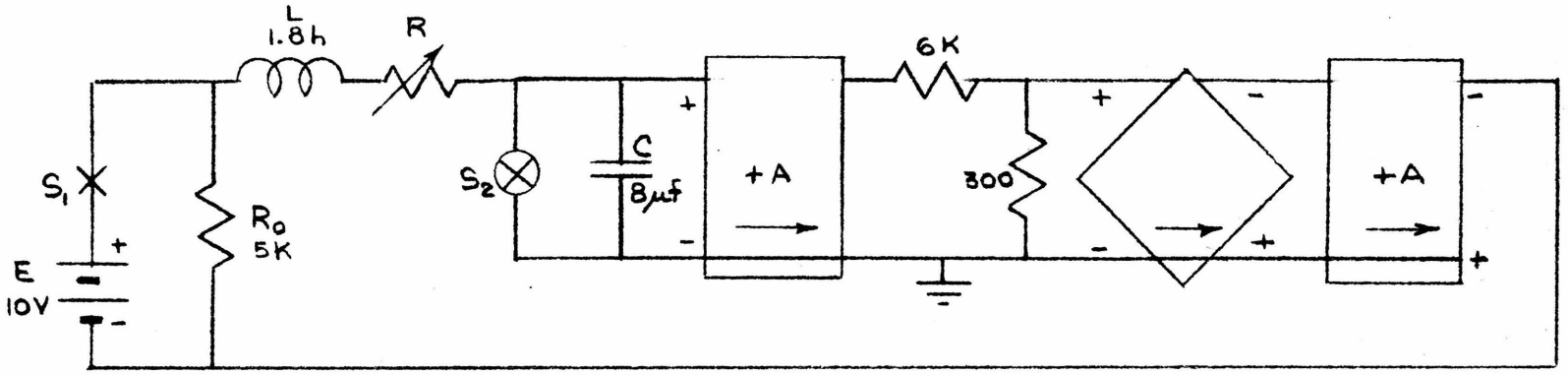

Symbols:

Synchronous switch, normally open

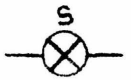

Synchronous switch, normally closed

Ancotron (arrow points toward output side)

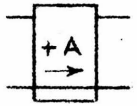

Amplifier with positive gain, i.e. output in phase with input (arrow shows direction of amplification)

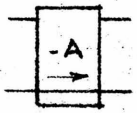

Amplifier with negative gain, i.e. output out of phase with input

Fig. 2.5 COMPLETE ANALOG FOR SYSTEM WITH NON-LINEAR CAPACITANCE

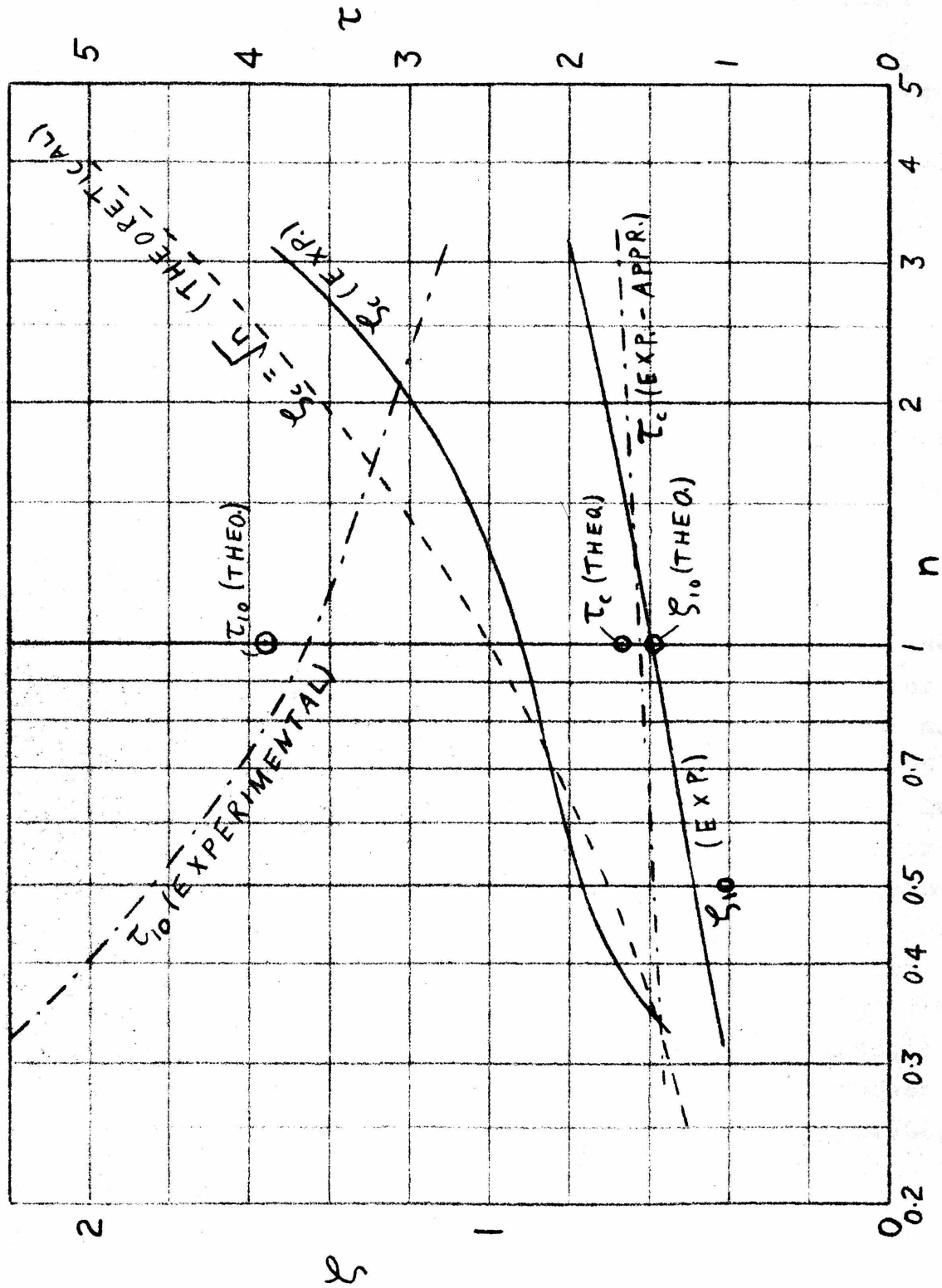

Fig. 2.6 RESULTS FOR NON-LINEAR CAPACITANCE
(See text for details)

made on an oscilloscope. To check the experimental method readings were also taken for a linear circuit and compared with the theoretical values on page 33. The results are summarized in the graph of fig. 2.6.

As derived in appendix C, the true value of ζ_c for these non-linear capacitances is

$$\zeta_c = \sqrt{n} \,. \qquad (2\text{-}15)$$

This curve is also plotted.

It will be seen that the experimental curve for ζ_c is not too close to the theoretical one. A major reason for the discrepancy is probably the difficulty of determining, by looking at an oscilloscope, when critical damping has been reached. The points for τ_c were found not to lie on a reasonable curve, and the line drawn here is merely an approximation. (In general the accuracy of time measurements suffered from a lack of precise calibration equipment.) The values for ζ_{10} and τ_{10}, however, were more consistent and reproducible.

As a further check numerical integration was used to see whether the experimental value of $\zeta_{10} = 0.72$ for $n = 2$ actually gives 10 % overshoot. The result was an overshoot of 9.4 % , the maximum occurring at $\tau = 3.35$ (compared to the experimental $\tau_{10} = 3.1$). Thus the value of ζ_{10} is as close as could be expected, since the error is only 0.5 % of $x_{max} = 1.100$. The value of τ is again low.

Finally, to check the behavior of the ancotron by itself, the exponent was obtained experimentally by plotting output versus input voltage, measured at dc, on log-log paper. The four actual values of n corresponding to $\frac{1}{3}$, $\frac{1}{2}$, 2 , and 3 are, respectively, 0.329, 0.504, 1.96, and 2.95.

7. Oscillograms *

Fig. 2.8, (a) to (c), shows some typical results for a non-linear capacitance, $n = 2$, with a step voltage suddenly applied. (a) is the charge, (b) the current, and (c) the "phase trajectory" which is included as a matter of theoretical interest.

The phase trajectory for a variable which is a function of time is a plot of the derivative of the function, as ordinate, versus the function itself, as abscissa. These coordinates constitute the "phase plane". The point corresponding to a given instantaneous state of the system, the "representative point", will move along the phase trajectory with time in a clockwise direction, if the usual sign conventions are observed.

In the case of damped oscillations the phase trajectory is some form of a spiral. For periodic (undamped) oscillations the trajectory is a closed curve, also known as a "limit cycle"; for it is the curve which the representative point will approach as a limit regardless of the starting point, assuming only one stable limit cycle to exist.

Phase trajectories are frequently used in theoretical work where it may be easier to solve for the trajectories than for the variable as a function of time. With the aid of the trajectory the function itself may then be found.

Fig. 2.8 (a) differs from the linear case chiefly in the lack of symmetry of the oscillations about the final steady-state value. Allowing for damping, the amplitude is considerably less above the steady-state value than it is below. This makes the phase trajectory

---

* The oscillograms as reproduced here are not sufficiently accurate to permit measurements to be taken from them, since the oscilloscope used had considerable distortion. They are intended to be illustrations only. Hence it was thought permissible to do some retouching for better reproduction.

appear flattened on the right.

2.8 (d) is the charge for a capacitance with $n = \frac{1}{2}$. Here the overshoot has a larger amplitude above the steady-state value than below. 2.8 (e) is similar to (d) except for the damping being less. (e) is to be compared with (f) which was taken for a linear system with the same frequency of oscillations and the same resistance as (e). The damping per cycle is much greater for the linear case.

8. Non-Linear Resistance

Fig. 2.4 shows a system containing a non-linear resistance to which a linear resistance R_1 has been added. The equation is

$$e = E\, f(t) = L\,\ddot{q} + R_1\dot{q} + V + \frac{q}{C} \qquad (2\text{-}16)$$

Proceeding as before let

$$v = R\cdot\dot{q}$$

$$\omega_o = \frac{1}{\sqrt{LC}}$$

$$x = \frac{\omega_o R_2}{v_o}\, q$$

$$\tau = \omega_o t$$

$$V = V_o\, \varphi\left(\frac{dx}{d\tau}\right)$$

$$K = \frac{V_o}{v_o}\,, \quad \text{where} \quad v = v_o \quad \text{when} \quad V = V_o$$

$$\zeta = \frac{KR_2}{2}\sqrt{\frac{C}{L}}$$

$$\eta = \frac{R_1}{2}\sqrt{\frac{C}{L}} = \frac{R_1}{KR_2}\,\zeta$$

Put $V_o = E$.

Then the equation becomes

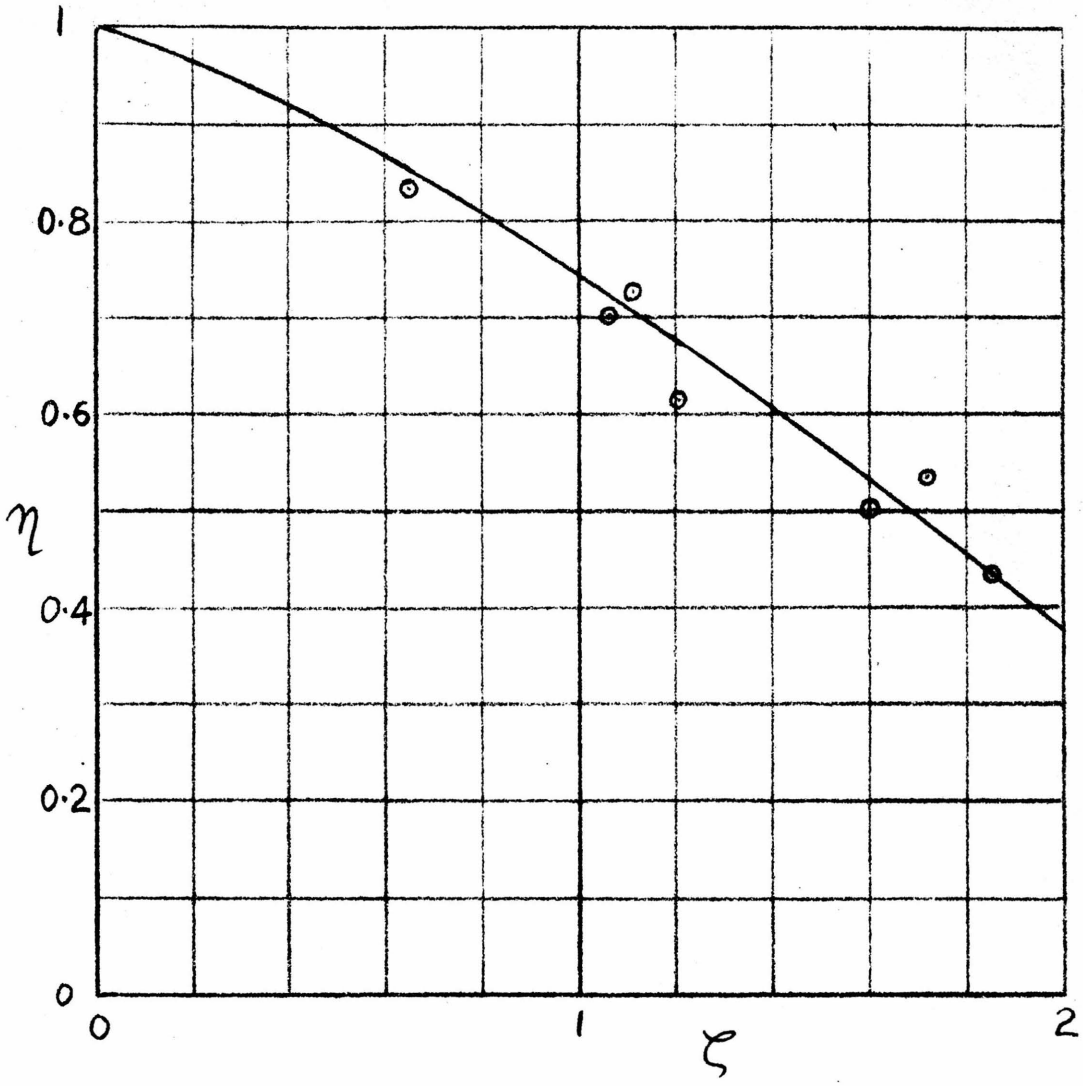

Fig. 2.7 RESULTS FOR SQUARE-LAW RESISTANCE

(Additional linear resistance η required for given square-law resistance ζ to produce critical damping)
⊙ - experimental values used for plotting graph

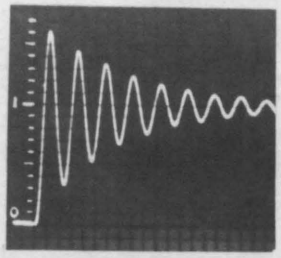

(a) CHARGE

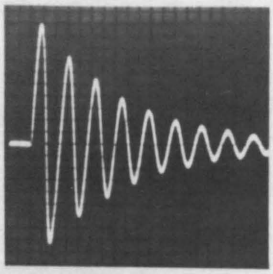

(b) CURRENT
CAPACITANCE, n= 2

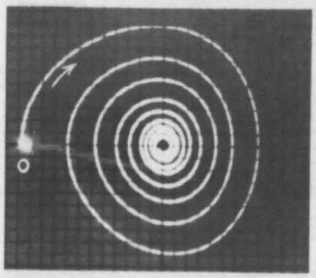

(c) PHASE TRAJECTORY

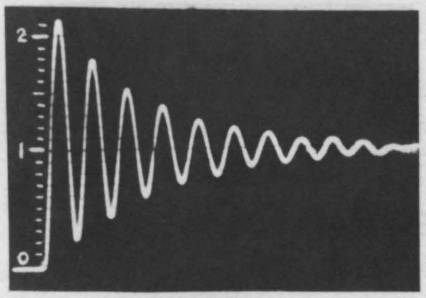

(d) CHARGE

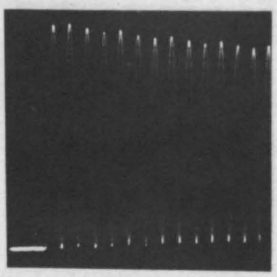

(e) CHARGE (LESS DAMPING)
CAPACITANCE, n= 1/2

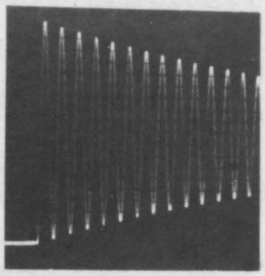

(f) CHARGE, SAME
FREQUENCY AS (e).
LINEAR

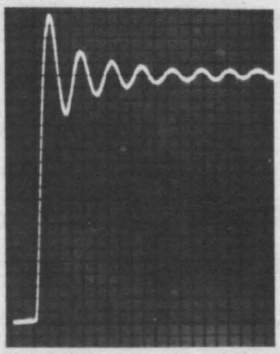

(g) CHARGE

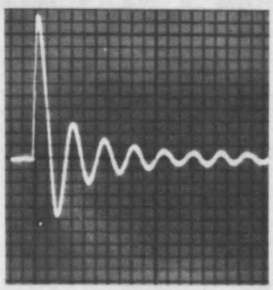

(h) CURRENT

RESISTANCE, n= 2

FIG. 2.8 NON-LINEAR ELEMENTS, STEP FUNCTION INPUT

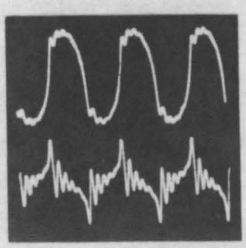

(a) WAVE FORM

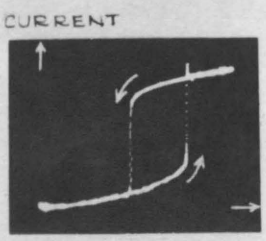

(b) CURRENT JUMP

FIG. 2.9 CAPACITANCE, n= 2
STEADY-STATE SINE WAVE

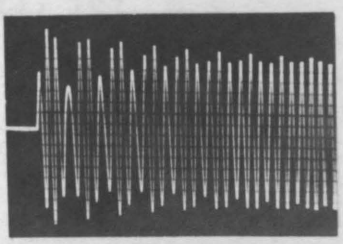

FIG 2.10 CAPACITANCE, n=2
SINE WAVE SUDDENLY APPLIED

$$f(\tau) = \frac{1}{2\zeta}\left(\frac{d^2x}{d\tau^2} + x\right) + \frac{\eta}{\zeta}\frac{dx}{d\tau} + \varphi\left(\frac{dx}{d\tau}\right) \qquad (2\text{-}17)$$

Without the linear damping term (if $\eta = 0$) the character of the solution would again be determined by the single parameter ζ.

Only the case $n = 2$ with a step function applied was investigated in some detail. If $n < 1$ the large slope at the origin tends to cause instability in the circuit. It was possible, however, to verify qualitatively that a non-linear resistance with $n < 1$ damps out oscillations more rapidly than a linear one, due to the high resistance when the current is small.

The oscillograms of Fig. 2.8 (g) and (h) show the charge and current for a non-linear resistance, $n = 2$, with a step voltage applied. It may be seen that the damping initially is very high. But as the current decreases the damping per cycle becomes very low; the oscillations die out much more slowly than for the linear circuit. In fact, it would seem that a condition of critical damping could not be achieved with only a non-linear resistance of $n > 1$. Regardless of how high the damping may be initially, by the time the current approaches zero the damping will have dropped to too low a value. Therefore a linear resistance was added to the circuit to provide damping at low values of current also.

The curve of Fig. 2.7 shows some quantitative results obtained. They give the additional linear resistance (η) required to give a critically damped response to a suddenly applied voltage as a function of the amount of non-linear resistance (ζ), for $n = 2$.

9. Steady-State Sinusoidal Input

In a linear circuit the response to a sinewave can only be another sinewave of the same frequency. The circuit can only change the amplitude and phase.

The behavior with a non-linear circuit is much more complex. Although a detailed study was not undertaken some of the more interesting effects, characteristic of many non-linear circuits, were investigated qualitatively, and Fig. 2.9 shows two oscillograms taken for the series circuit with a capacitance having $n = 2$.

Fig. 2.9 (a) gives the charge (top) and current (bottom) in a circuit having a resonant frequency of the order of ten times the applied frequency. The waveform is approximately that of a sinewave with damped oscillations, at a frequency about ten times as high, superimposed.

As resonance is approached the waveform of the response becomes more nearly sinusoidal. If the damping is high the current will simply go through a maximum at some frequency near $\omega_o = 1/\sqrt{LC/K}$ (see page 37), the exact frequency depending on the magnitude of the applied voltage.

If the damping is low, however, the current, which at first increases considerably as the frequency is raised, will suddenly jump to a lower value.[10] Also if at a fixed frequency in that region the voltage is increased the current will suddenly jump to a higher value at some voltage; on decreasing the voltage, the current will again jump to a lower value but this occurs at a lower voltage than before.

Fig. 2.9 (b) is an interesting oscillogram giving the amplitude of the current as a function of the amplitude of the input voltage. It was obtained by rectifying both before applying them to a dc oscilloscope. The input voltage was slowly varied manually from zero to a maximum

and back to zero while taking a time exposure of the oscilloscope screen.

The oscillogram shows the current to be a double-valued function of the applied voltage. The upper and lower branch are actually connected by a curve with a negative slope, but if the voltage source has a low impedance this connecting branch is unstable, and the current will jump between the lower and the upper branch discontinuously.[11] If, however, the circuit had been supplied from a high-impedance current generator and the voltage had been measured, the connecting branch would have been stable and would have shown up in the oscillogram.

The small pip evident at the top of the ascending jump is due to a transient overshoot.

10. Sinusoidal Input Suddenly Applied

Using the same circuit as above, fig. 10 is the current obtained for a suddenly applied frequency in the vicinity of circuit resonance. A transient change in amplitude at a subharmonic frequency of about one-third the applied frequency is observed.

This may be considered to be a beat between the applied frequency and the frequency of the transient caused by the sudden excitation.[12] The beat dies out at a rate depending on the damping.

III SELF-OSCILLATING SYSTEMS WITH ONE DEGREE OF FREEDOM

1. Introduction

The theory of linear circuits is completely inadequate for analyzing the behavior of oscillators. In fact an oscillating circuit that is linear, even to the first approximation, over the entire range of the variables is a physical impossibility; it is the non-linear element that establishes the amplitude of oscillation as well as influencing frequency and waveform.

The simplest differential equation which adequately describes the main features of many oscillator circuits is the well-known Van der Pol Equation. It has been investigated analytically and graphically by Van der Pol and several other writers.[13,14,15,16,17,18,19] (Le Corbeiller, reference 15, gives a good general survey of the subject.) The derivation of the equation, including the necessary assumptions, is given in appendix D for a transformer-coupled oscillator (Fig. 3.1) and in appendix E for a multivibrator (Fig. 3.2).

Van der Pol's equation was chosen for study because solutions are available for special cases to check the results obtained. But other systems are just as easily set up on the computer, and some examples are given.

Van der Pol considered two types of oscillating systems. The first has only a single state of equilibrium, one of periodic oscillations, which it will reach from rest or any other initial conditions. This is an oscillator with "soft excitation". The system has a negative linear and a positive cubic damping term.

The other system contains a positive linear, a negative cubic, and a positive fifth-order term. It is stable both at rest and in a state of steady oscillations. The oscillations may be shock-excited but will not start

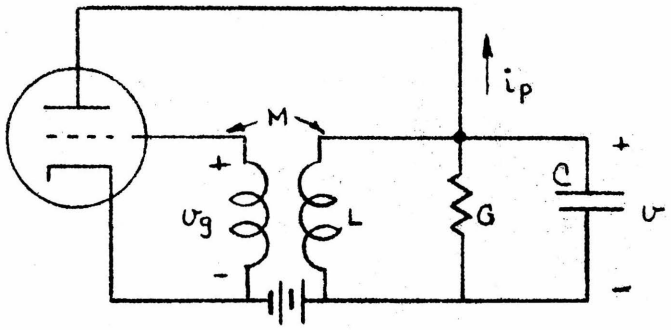

Fig. 3.1 PLATE-TUNED TRANSFORMER-COUPLED OSCILLATOR

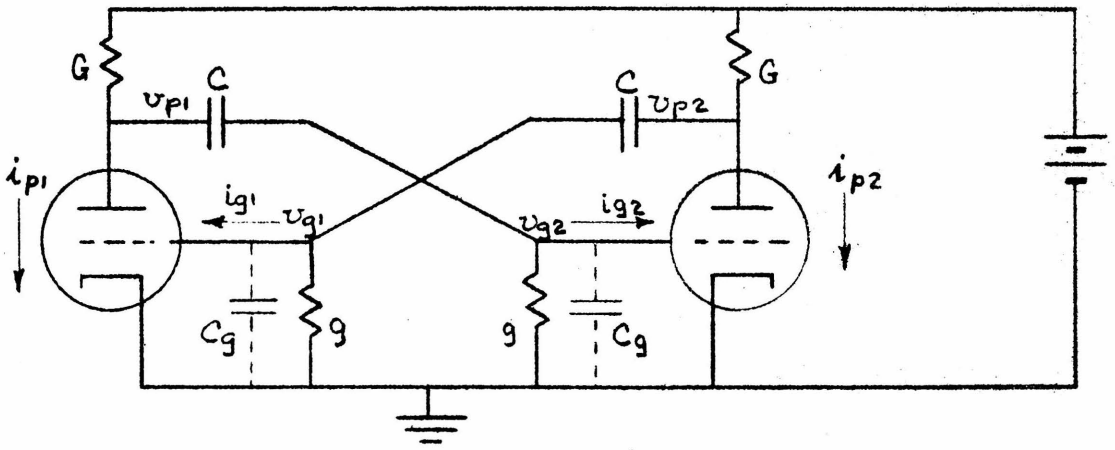

Fig. 3.2 SYMMETRICAL MULTIVIBRATOR

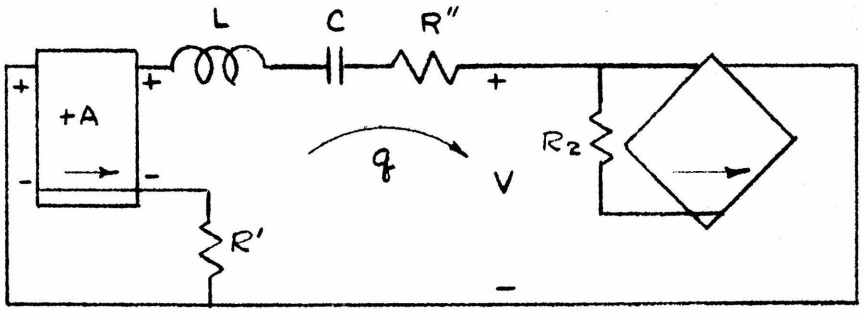

Fig. 3.3 ANALOG FOR VAN DER POL'S EQUATION

by themselves. This method of starting oscillations is known as "hard excitation". Oscillators may not often be found to behave in this manner, but the phenomenon is well-known to those who experiment with high-gain amplifiers. Such amplifiers are frequently stable by themselves but will start oscillating when a signal is applied and continue to oscillate even though the signal is removed again.

The system with soft excitation was studied in some detail; also an example of a system with hard excitation was set up which is somewhat different from Van der Pol's.

2. Analog for Van der Pol's Equation

The analog used is shown in Fig. 3.3. The circuit is actually that of Fig. 2.4 if we put $e = 0$ and $R_1 = -(A - 1)R' + R''$, where R'' includes coil losses and any other linear positive resistance present in the circuit.

Again let $\zeta = \frac{KR_2}{2}\sqrt{\frac{C}{L}}$, and $\eta = \frac{R_1}{2}\sqrt{\frac{C}{L}}$. Then from equation (2-16)

$$\frac{1}{2\zeta}\left(\frac{d^2x}{d\tau^2} + x\right) + \frac{\eta}{\zeta}\frac{dx}{d\tau} + \varphi\left(\frac{dx}{d\tau}\right) = 0 \qquad (3\text{-}1)$$

For Van der Pol's equation a cube-law pattern is used so that $\varphi\left(\frac{dx}{d\tau}\right) = \left(\frac{dx}{d\tau}\right)^3$.

If A is large enough, η and R_1 are negative. Hence let $\mu = -2\eta$. Also introduce a new variable $z = \sqrt{\frac{6\zeta}{\mu}}\,x$. This gives Rayleigh's Equation

$$\frac{d^2z}{d\tau^2} - \mu\left[\frac{dz}{d\tau} - \frac{1}{3}\left(\frac{dz}{d\tau}\right)^3\right] + z = 0 \qquad (3\text{-}2)$$

Differentiating with respect to τ and letting $u = \frac{dz}{d\tau} = \sqrt{\frac{6\xi}{\mu}} \frac{dx}{d\tau}$ we have Van der Pol's Equation

$$\frac{d^2u}{d\tau^2} - \mu(1 - u^2) \frac{du}{d\tau} + u = 0 \qquad (3\text{-}3)$$

As shown in appendixes D and E, it is the variable u or the current i in the analogous circuit which corresponds to the output voltage of an oscillator. The important relations are summarized below:

$$u = \sqrt{\frac{3KR_2}{-R_1}} \frac{i}{i_o} \qquad R_1 = -\left[(A - 1) R' - R''\right]$$

$$\mu = -R_1 \sqrt{\frac{C}{L}} \qquad V = V_o \left(\frac{i}{i_o}\right)^3$$

$$\tau = \frac{t}{\sqrt{LC}} \qquad K = \frac{V_o}{i_o R_2}$$

(i_o, V_o) are the reference values for the cube-law resistance element.

3. Results

Both the frequency and amplitude of the steady-state oscillations were measured as a function of the parameter μ and the results are plotted in Fig. 3.4. The frequency is plotted both in terms of $\frac{f}{f_o}$ and $\frac{\mu}{\pi} \frac{f}{f_o}$ to verify theoretical predictions. As has been shown by several authors[14,15,17,18] the limiting values should be

$$\mu \to 0 \ , \quad \frac{f}{f_o} \to 1.00$$

$$\mu \to \infty, \quad \frac{\mu}{\pi} \frac{f}{f_o} \to \frac{2}{3 - 2 \ln 2} = 1.24$$

The results appear to agree with the theoretical values.

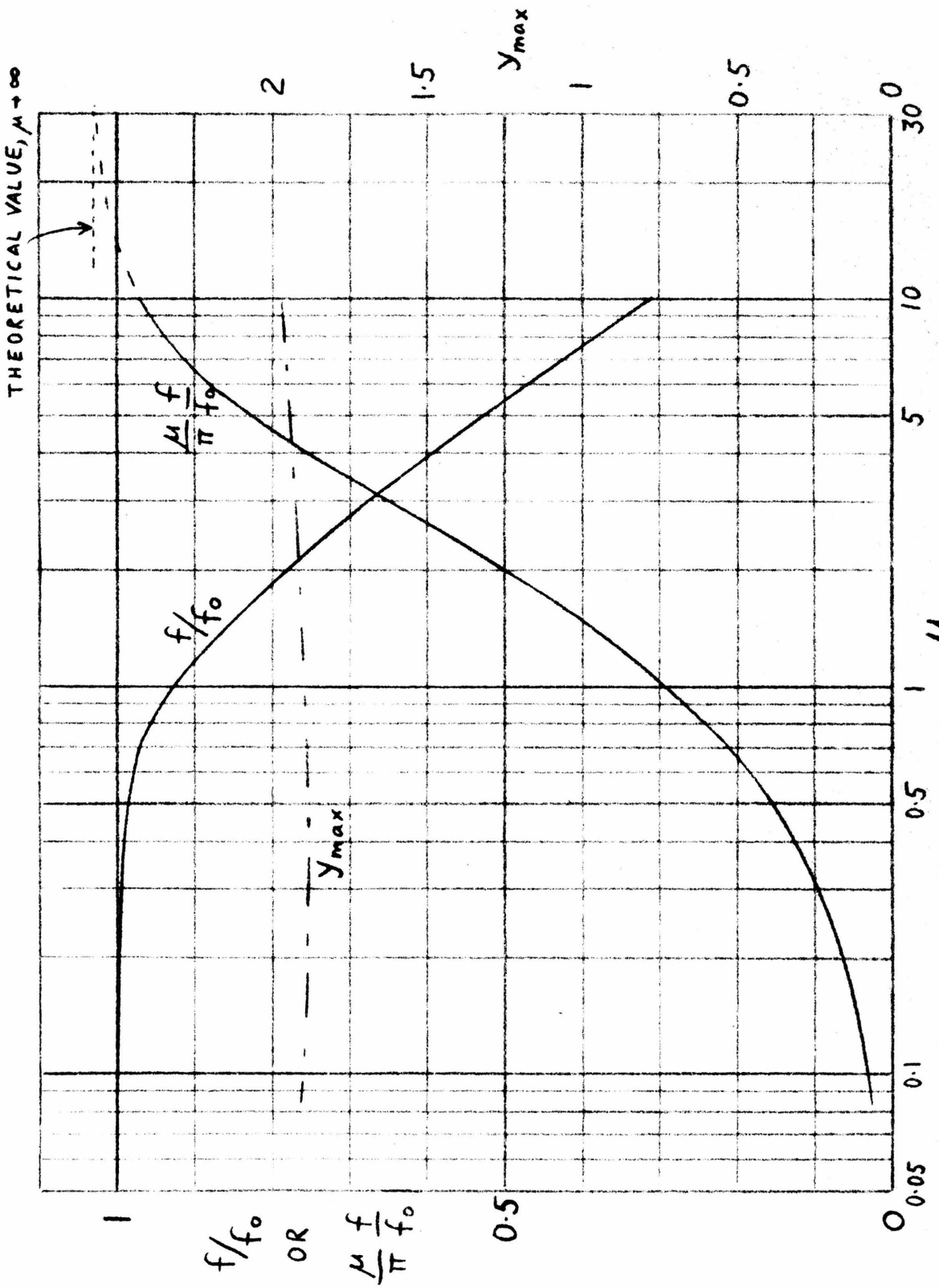

FIG. 3.4 RESULTS FOR VAN DER POL'S EQUATION

The amplitude u_{max} is also plotted. Over the entire range $0.1 < \mu < 10$ it is seen to vary by less than 7 % from the value 2.00 . Theory predicts $u_{max} = 2$ for both very large and very small values of μ . Due to lack of accuracy in the equipment used for measuring the amplitude, this curve may be in error by a few percent.

4. Oscillograms

Van der Pol originally determined by the method of isoclines the phase trajectories, and from this the waveforms, of the oscillations for $\mu = 0.1$, 1, and 10.[14] These by now classical diagrams have since been reprinted by several writers.[16,17,19] It was thought interesting to try to reproduce them on the computer, and the results are Figs. 3.5, (a) to (c).

Both the growth of oscillations from the time the circuit is closed (the initial point is marked o) and the phase trajectory are shown in each case. The phase trajectories only show the representative point approaching the limit cycle from the origin. The scales for the dimensionless variables $\frac{du}{d\tau}$ and u were made approximately the same on each diagram, but the three diagrams are not shown to the same scale. Some of the original oscillograms do not reproduce well since the changing velocity of the beam produces a wide range of exposures. Some retouching was necessary.

There is seen to be general agreement between these pictures and Van der Pol's diagrams. His diagrams for $\mu = 0.1$ are probably not too accurate due to the great labor involved in obtaining by graphical methods the large number of cycles required for the system to reach the final amplitude.

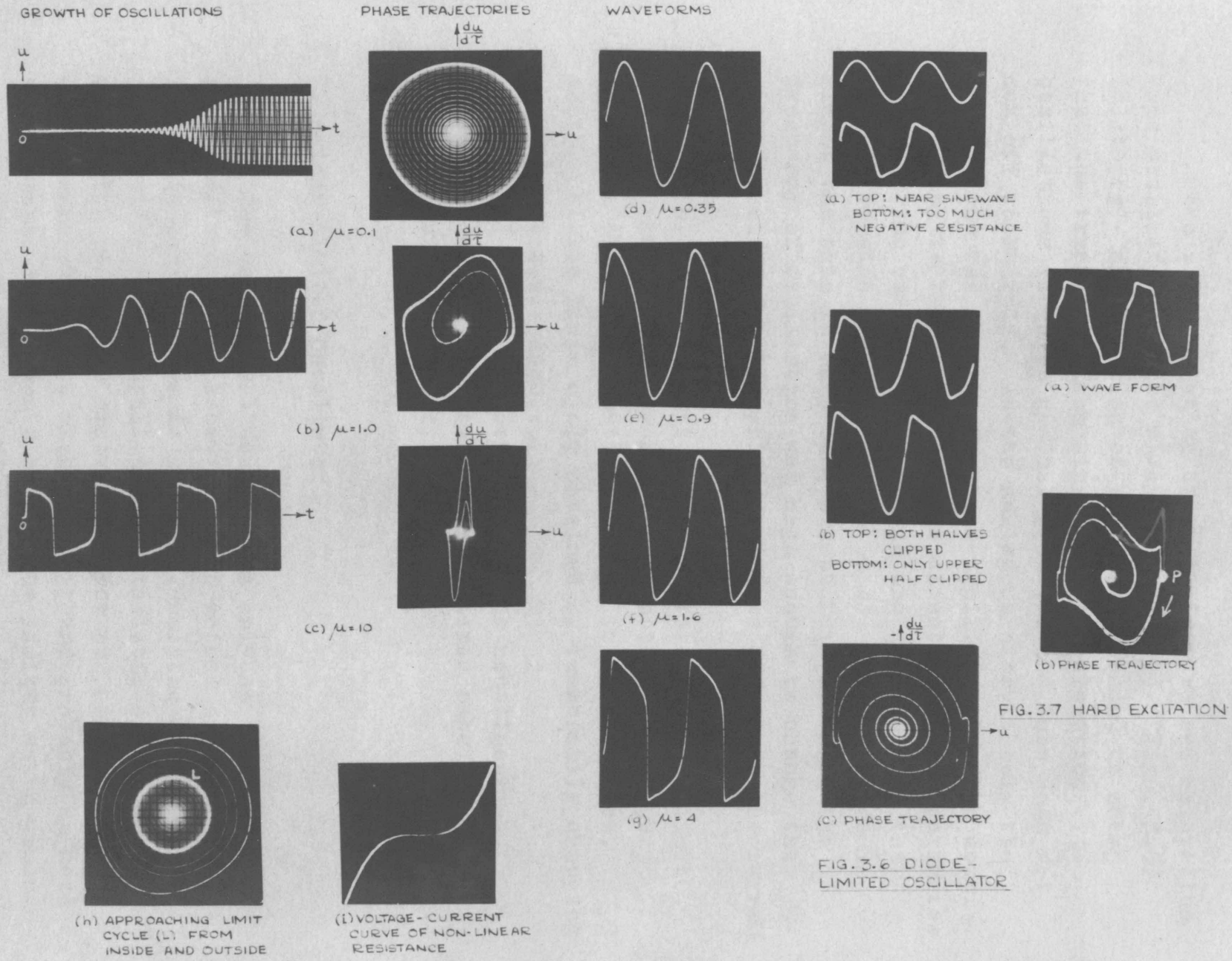

FIG. 3.5 VAN DER POL'S EQUATION
(SOFT EXCITATION)

FIG. 3.7 HARD EXCITATION

FIG. 3.6 DIODE-LIMITED OSCILLATOR

The close relation between sinewave and relaxation type oscillators is not always appreciated. Figs. 3.5, (d) to (g) are a series of pictures intended to show that the transition from sinusoidal to relaxation oscillations is quite gradual provided the tube does not cut off too sharply. In the analogous circuit only the capacitance was changed from one oscillogram to the next. (According to the equations this affects only the parameter μ, not the variable u. Hence the amplitude of the current remains proportional to u.) The amplitude is almost the same in each case except for (d) where the frequency of oscillation was high enough to change the coil losses materially which of course decreases the current somewhat.

(h) is an attempt to demonstrate that the limit cycle, marked L, will be approached both from inside (here the origin) and outside (here, for convenience, another stable limit cycle obtained by temporarily changing the circuit resistance).

(i) shows the behavior of the non-linear resistance during operation. The desired cube law is followed quite accurately.

5. Diode-Limited Oscillator

The Van der Pol equation is only an idealized approximation to the behavior of an actual oscillator. The cubic damping term is a simple analytic device for representing the saturation characteristic of the vacuum tube which limits the amplitude. For purposes of experimental studies a much simpler, and probably no more approximate, device would be a diode limiter which would prevent the current or voltage from exceeding a certain value.

Such a scheme actually makes also a very practical oscillator with constant amplitude of oscillation. A diode voltage-limiter,of the type used in Fig. 4.7, is placed in the grid circuit of a vacuum-tube oscillator to limit the grid voltage excursion, and it is set to keep the tube operating on the linear part of its characteristic. The voltage departs from a sinewave at the peaks only, and this gives rise to harmonics of a high order which are easily filtered. Furthermore, the distortion can be kept small by proper adjustment.

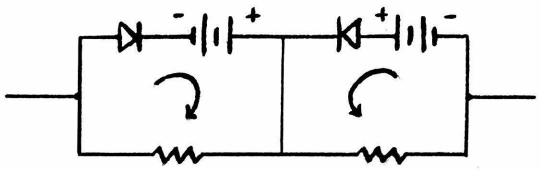

Fig. 3.8 CURRENT LIMITER

An analogous circuit was set up by replacing the cube-law resistance element (including the ancotron) by a simple current limiter as in Fig. 3.8. Fig. 3.6 shows some oscillograms. The upper curve of 3.6 (a) indicates an almost pure sinewave obtained by setting the negative resistance to a value just above that necessary to start oscillations. The lower curve shows the effect of increasing the negative resistance (making it more negative).

3.6 (b) shows the difference between clipping both the positive and negative parts of the cycle (top) and clipping only one half (bottom), all other conditions being the same. The negative resistance was increased to a point of excessive distortion to exaggerate the difference which would normally be hardly noticeable. Evidently only one diode limiter is needed, resulting in greater economy and ease of adjustment with little increase in distortion.

The distortion was actually measured on a distortion analyzer with the negative resistance adjusted to a lower value, just above the minimum which would give really stable oscillations. With symmetrical clipping the

total distortion was 0.37 % ; with clipping on only one side the distortion rose to 1.35 % .

It is interesting to note that a change in the level at which the current is limited produces only a change in amplitude and does not affect frequency or waveform. This makes an effective volume control which might also be adapted to automatic operation.

A typical phase trajectory is shown in (c) for a circuit with two symmetrical clippers and considerable distortion.

6. Hard Excitation

To produce a system with hard excitation as described by Van der Pol an additional fifth-order damping term is required. Since only one ancotron was available, such a system could not be set up. Instead the current limiter was again used to provide saturation. To have a negative cubic term the ancotron polarity was reversed from that used for the earlier scheme. The linear term has to be positive now, hence a resistor suffices.

For small currents the positive linear resistance is the only damping term which has any effect. Therefore the system will not start oscillating by itself but will remain at rest. If the initial current is made large enough, however, the negative cube-law resistance overcomes the positive damping and causes the current to grow further, The oscillations will increase until their growth is stopped by the limiter (or Van der Pol's quintic damping).

Thus the system as represented in the phase plane has two stable positions, one the origin and the other the limit cycle corresponding to stable oscillations. The system may be transferred from the first to the second state by shock or "hard" excitation. Another way is to

start with a sufficiently large dc current. The latter method was used here. The condenser was first shorted out, and a dc current was made to flow by unbalancing the output amplifier of the ancotron circuit. When the short was removed the system would oscillate. The dc voltage was blocked by the condenser during operation.

A typical waveform is shown in Fig. 3.7 (a). Distortion is much higher here, and this sytem would not seem to have many practical applications.

3.7 (b) shows the phase trajectory for a borderline case. The initial current with the condenser shorted caused the system to start off at point P. As soon as the short was removed the system began to go around the limit cycle (outer curve). But after one brave revolution the system decided it was not strong enough to continue on the merry-go-round, and it collapsed toward the origin. Thus in a single diagram both the ordinarily stable states are represented.

IV STATIC AND DYNAMIC FRICTION IN SIMPLE POSITION SERVO

1. Introduction

The problem of "dry" friction in moving systems is usually simplified by assuming the friction force to be of constant magnitude and directed such as to oppose the motion. This so-called Coulomb friction has been investigated both theoretically[20,21] and by Analog Computer methods[22]. The electrical analog of a Coulomb friction element is simply a voltage limiter consisting of diodes and batteries.

Actually, the friction force is known usually to be greater when the system is standing still than when it is in motion. That is, a stationary system can have a friction force preventing the start of motion up to a maximum value S which we shall call "static friction", a term that has been aptly abbreviated to "stiction"; once the system is moving the friction drops to a value D to be called "dynamic friction" (this is the Coulomb friction)*. The magnitude of D will again be assumed to be independent of velocity.

It will also be assumed that the friction F drops suddenly from the value S to D as soon as the velocity departs from zero. Thus the graph of the idealized friction force (or torque) F versus velocity is as shown in Fig. 4.1.

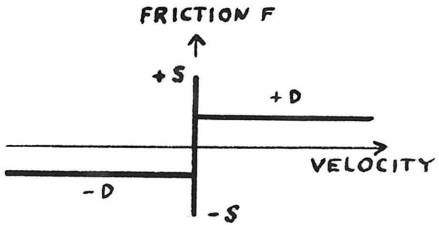

Fig. 4.1 STATIC (S) AND DYNAMIC (D) FRICTION

By dissipating energy friction usually serves to damp out oscillations and thus increase the stability of

---

* A one-word name for Coulomb friction has apparently not yet been coined. An appropriate term might be "sliption".

a system. But the presence of static friction which is greater than the dynamic friction may, in some cases, actually lead to instability. Many mechanical systems which are insufficiently lubricated are found to "chatter" or "shimmy". The reader is referred to Den Hartog[23] for a qualitative discussion of several practical examples.

Sometimes the effect is desirable. Thus the bowing of string instruments depends on the presence of stiction which is purposely increased by the application of rosin. The action is analogous to that of a vacuum-tube oscillator. The power is provided by the steady pull on the bow, and the friction characteristic provides the negative resistance.

Chattering may be particularly annoying in position servomechanisms, and this example is treated in detail below. The subject seems to have received relatively little attention in the literature.[24,25]

2. Analog of Position Servo[22]

Let θ be the shaft angle of the servo motor which has a moment of intertia J, a linear (viscous) damping coefficient B, and a dry-friction torque F. Let the servo be required to follow an angle θ_i. Assume the motor torque T to be proportional to the error angle $\theta_i - \theta$, time delays due to inductance in the armature and field circuits being neglected, so that

$$T = K (\theta_i - \theta) \tag{4-1}$$

Then the equation of the rotating system is

$$K (\theta_i - \theta) = J \ddot{\theta} + B \dot{\theta} + F \tag{4-2}$$

or

$$K \theta_i = J \ddot{\theta} + B \dot{\theta} + K \theta + F \tag{4-3}$$

(Note that this equation also applies to a simple

mechanical system consisting of a mass, a spring, viscous and dry friction, if θ is the displacement and a force $K\,\theta_i$ is applied.)

Analogous circuits are shown in Fig. 4.2.

3. Analysis of Position Servo Following a Constant Velocity

Let

$$K\,\theta_i = M\,t \tag{4-4}$$

so that M/K is the constant velocity to be followed.

The system can be replaced by a linear one having a moment of inertia J, a viscous friction B, and a spring constant K, to which a net torque $K\,\theta_i - F$ is applied. This torque, as shown in Fig. 4.3, remains zero, since the stiction opposes the torque $K\,\theta_i$, until $K\,\theta_i$ equals the maximum stiction torque S, at a time $t_1 = S/M$. The angle θ also remains zero until then. At $t = t_1$ the friction F suddenly drops to D and motion starts.

For $t > t_1$, the linear system has applied to it a net torque $M\,t - D = M\,(t - t_1) + S - D$ and equation (4-3) becomes

$$M\,(t - t_1) + S - D = J\,\ddot{\theta} + B\,\dot{\theta} + K\,\theta \tag{4-5}$$

Equation (4-5) continues to apply unless the velocity θ drops to zero. In that case the system sticks, that is, the velocity remains zero for a while. Suppose sticking occurs at $t = t_2$. Then the system will remain stationary until the error torque exceeds S again at some time t_3 at which $K\,\theta_i\big|_{t=t_3} - K\,\theta\big|_{t=t_2} = S$. After that the system moves again according to equation (4-5) with t_1 replaced by t_3 and θ replaced by $\theta - \theta\big|_{t=t_2}$.

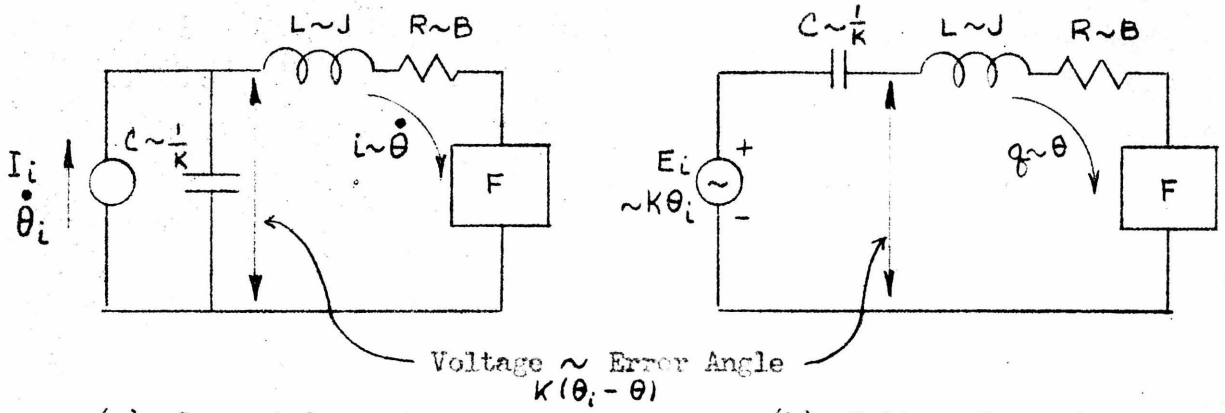

(a) Current Generator (b) Voltage Generator

Fig. 4.2 POSITION SERVO ANALOGS

F is element representing dry friction ~ means 'analogous to'

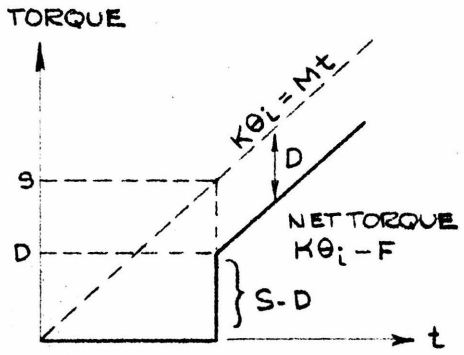

Fig. 4.3 NET TORQUE APPLIED TO LINEAR SYSTEM

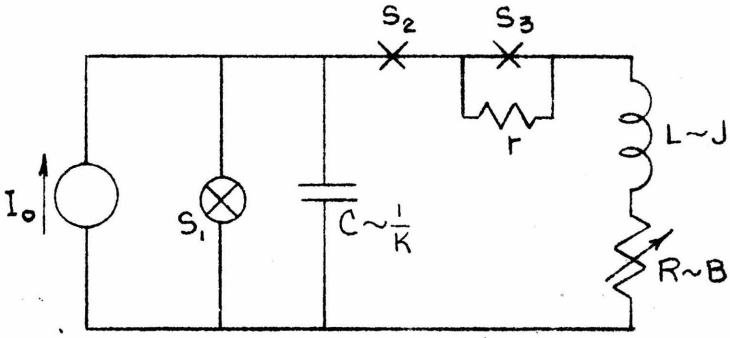

Fig. 4.4 ANALOG FOR OBTAINING CRITICAL CONDITIONS

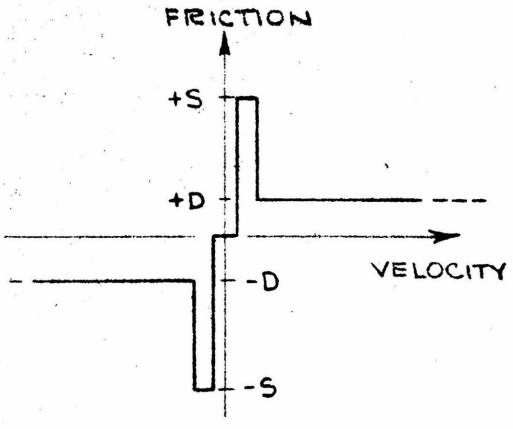

(a) Transfer Function

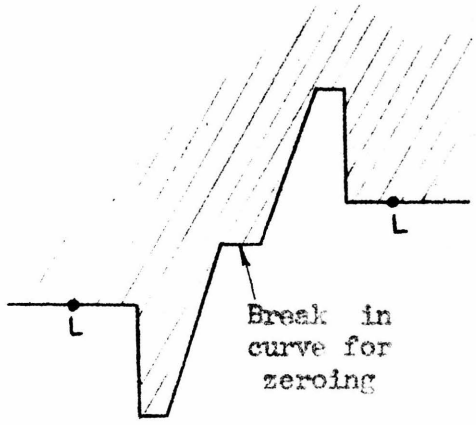

(b) Ancotron Pattern

Fig. 4.5

Not only does the same equation apply, but the initial conditions at t_3 are also the same as at t_1 if we subtract the angle $\theta\big|_{t=t_2}$ from θ. If the system stops once, it will stop again, and the chattering is a periodic phenomenon.

If, however, the velocity $\dot{\theta}$ does not return to zero after $t = t_1$ the system cannot stick. The oscillations die out, and the system will eventually follow at the same constant velocity M/K as the input, except for a constant error angle $D + BM/K$.

Thus the behavior can be predicted by solving equation (4-5) and finding the condition for $\dot{\theta} = 0$. The equation itself is easily solved.

Let

$$\omega_o = \sqrt{\frac{K}{J}}$$

$$x = \frac{\omega_o K}{M}\,\theta$$

$$\sigma = \frac{\omega_o}{M}\,S$$

$$\delta = \frac{\omega_o}{M}\,D$$

$$\lambda = \sigma - \delta = \frac{\omega_o}{M}\,(S - D)$$

$$\tau = \omega_o\,(t - t_1) = \omega_o t - \sigma$$

$$\zeta = \frac{1}{2}\,\frac{B}{\sqrt{JK}}$$

Then equation (4-3) can be written

$$\tau + \lambda = \frac{d^2x}{d\tau^2} + 2\zeta\frac{dx}{d\tau} + x \qquad (4\text{-}6)$$

Solving by Laplace transforms:

$$\mathcal{L}(\tau) = \frac{1}{s^2} \qquad \text{and} \qquad \mathcal{L}(\lambda) = \frac{\lambda}{s}$$

Hence

$$x(s) = \frac{\frac{1}{s^2} + \frac{\lambda}{s}}{(s + \zeta)^2 + (1 - \zeta^2)} \qquad (4\text{-}7)$$

From transform pairs 2.601 and 1.304 in Gardner and Barnes[7] the solution is

$$x(\tau) = \tau + (\lambda - 2\zeta) - \frac{e^{-\zeta\tau}}{\sqrt{1-\zeta^2}} \left\{ \left[1 + \zeta(\lambda - 2\zeta) \right] \sin\left(\sqrt{1-\zeta^2}\,\tau\right) + (\lambda - 2\zeta)\sqrt{1-\zeta^2}\, \cos\left(\sqrt{1-\zeta^2}\,\tau\right) \right\} \tag{4-8}$$

Also

$$\frac{dx}{d\tau} = 1 + e^{-\zeta\tau}\left[\frac{\lambda - \zeta}{\sqrt{1-\zeta^2}} \sin\left(\sqrt{1-\zeta^2}\,\tau\right) - \cos\left(\sqrt{1-\zeta^2}\,\tau\right) \right] \tag{4-9}$$

$$\frac{d^2x}{d\tau^2} = e^{-\zeta\tau}\left[\frac{1-\lambda\zeta}{\sqrt{1-\zeta^2}} \sin\left(\sqrt{1-\zeta^2}\,\tau\right) + \lambda \cos\left(\sqrt{1-\zeta^2}\,\tau\right) \right] \tag{4-10}$$

4. Critical Conditions

The critical value of λ for a given ζ is that for which the velocity just goes to zero, i.e. $\frac{dx}{d\tau} = \frac{d^2x}{d\tau^2} = 0$. Using the subscript c for these critical conditions one obtains a set of equations:

$$\left.\begin{aligned} \lambda_c^2 - 2\lambda_c\zeta_c + 1 &= e^{2\zeta_c\tau_c} \\ \tan\left(\sqrt{1-\zeta_c^2}\,\tau_c\right) &= \frac{\lambda_c\sqrt{1-\zeta_c^2}}{\lambda_c\zeta_c - 1} \end{aligned}\right\} \tag{4-11}$$

Solutions for some special cases, obtained by trial-and-error methods, are tabulated below.

$\sqrt{1-\zeta_c^2}\,\tau_c$	ζ_c	λ_c
2π	0.000	0.000
$7\pi/4$	0.055	0.947
$3\pi/2$	0.264	3.78
$5\pi/4$	0.714	56
π	1.000	∞

It can be seen from these results that a servo following a constant-velocity input will chatter only if

(1) static friction exists which is greater than the dynamic friction by a certain amount (i.e. $\lambda \geq \lambda_c$),

(2) linear (viscous) friction by itself is less than critical (i.e. $\zeta < 1$).

Also, if the linear (viscous) friction is very small, the system is almost certain to chatter since some stiction is unavoidable. With a given amount of static, dynamic, and viscous friction there is a minimum velocity which the system can follow without chattering since λ_c is proportional to the reciprocal of the velocity.

Thus stiction may have the effect of making a system unstable even though it has some viscous damping. Physically the instability is due to the sudden force or torque, S - D , applied to the system when it is ready to move.

Dynamic (Coulomb) friction alone does not produce such an effect if the velocity to be followed remains constant. If the input velocity changes, such as in the case of a sinusoidal variation, chattering may occur over part of the cycle with only dynamic friction, since the output velocity is forced to go through zero.[22]

5. Computer Solutions for Critical Conditions with Constant-Velocity Input

Instead of solving equation (4-11) directly, a linear circuit corresponding to equation (4-6) was set up as shown in Fig. 4.4.

At the start of the cycle switch S_3 is already closed, but S_2 is open. S_1 opens to begin charging C with the constant current I_o . This current corresponds to the constant input velocity. At a time $t' = \frac{S - D}{M} = \frac{\lambda}{\omega_o}$ switch S_2 closes. This is the start of the solution of

equation (4-11), for the initial voltage $\frac{I_o \lambda}{C\omega_o}$ on the condenser corresponds to the sudden torque S - D applied to the system when motion starts (see Fig. 4.3).

After a sufficient time has elapsed, switch S_3 opens, S_1 closes shortly after, and S_2 remains closed. A large resistance r is thus inserted to cause a rapid decay in the current. S_2 then opens, S_3 closes, and the cycle can start over again.

To find a solution for a given value of resistance R , the delay time t' is varied until the voltage across R , as observed on an oscilloscope, just goes to zero, with zero slope, after the first cycle of oscillation. This corresponds to the critical condition (see section 4). By measuring the time delay and knowing L, R, and C the values of ζ_c and λ_c can be calculated. The resultant curve is plotted in Fig. 4.6, together with the calculated values on page 65 and values obtained from the direct analog (see below).

6. Ancotron Analog for the Complete System

The assumed friction characteristic of Fig. 4.1 is a multi-valued function at the origin. This function is here approximated by the single-valued function of velocity shown in Fig. 4.5 (a).

The actual pattern is that of Fig. 4.5 (b). The gain of the horizontal deflection circuit was made high so that the center of the pattern would be traversed rapidly. To avoid going over the edge of the pattern, voltage limiters were used which stopped the beam at the positions labeled L . Since the output voltage remains constant beyond these points the effect of the high gain is to compress the pattern so that the velocity differs

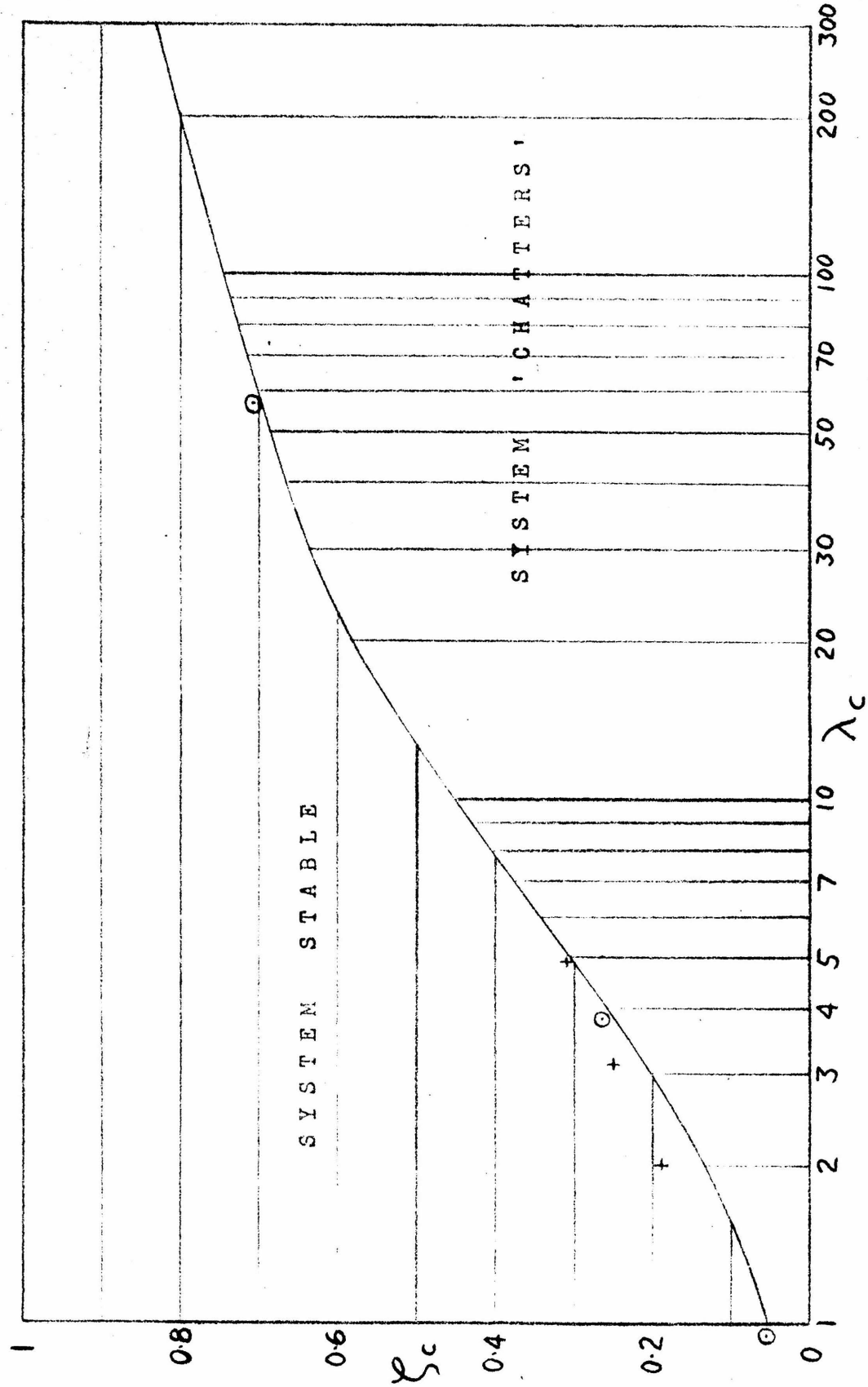

Fig. 4.6 CRITICAL CURVE FOR POSITION SERVO. CONSTANT-VELOCITY INPUT IN PRESENCE OF STATIC, DYNAMIC, AND VISCOUS FRICTION

⊙ Points computed from equations
\+ Points obtained by direct analog method using ancotron

only little from zero as the output varies from O to S to D .

The actual transfer function, which is photographed in Fig. 4.9 (c), thus can approximate Fig. 4.1 as closely as desired, except for the fact that when the velocity returns to zero the friction force must go from D to S first before dropping to zero. This does not occur in a physical system, but the difference is negligible as the duration of this "pip" is so short that it takes no appreciable energy out of the system. The analogy, however, breaks down when the maximum velocity reached during a cycle is small.

The complete circuit is shown in Fig. 4.7. C' and C" are large integrating condensers used to observe voltages corresponding to input angle (angle to be followed) and output (shaft) angle of the servo. C" must be very large to avoid changing the solution; it is best shorted out when not in use. S_1 is the main timing switch; S_2 and S_3 serve to discharge the condensers after each on-period. Limiter 1, consisting of two crystal diodes and two equal batteries, limits the horizontal excursion of the beam; limiter 2, similar to limiter 1, permits reducing the value of S by clipping the peaks of the ancotron output voltage at a level equal to the adjustable battery voltages in the limiter. By changing these voltages and adjusting the gain of amplifier A_3 both S and D may be varied over a wide range.

7. Results for a Constant-Velocity Input

The results obtained with the ancotron are summarized in the oscillograms of Fig. 4.9. The accuracy of these pictures again suffers somewhat due to distortion in the oscilloscope used.

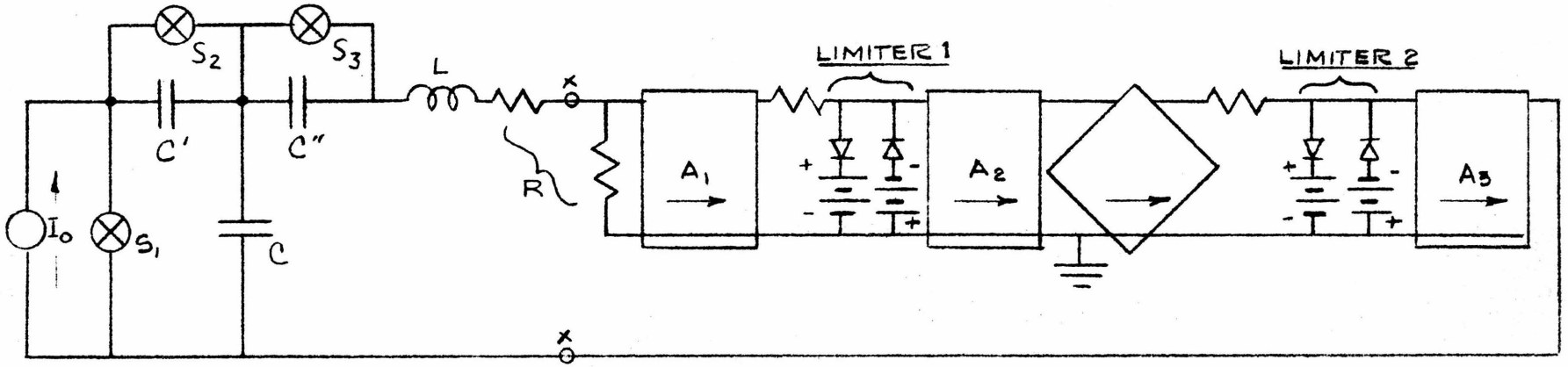

Fig. 4.7 ANCOTRON ANALOG, COMPLETE
(See fig. 2.5 for special symbols)

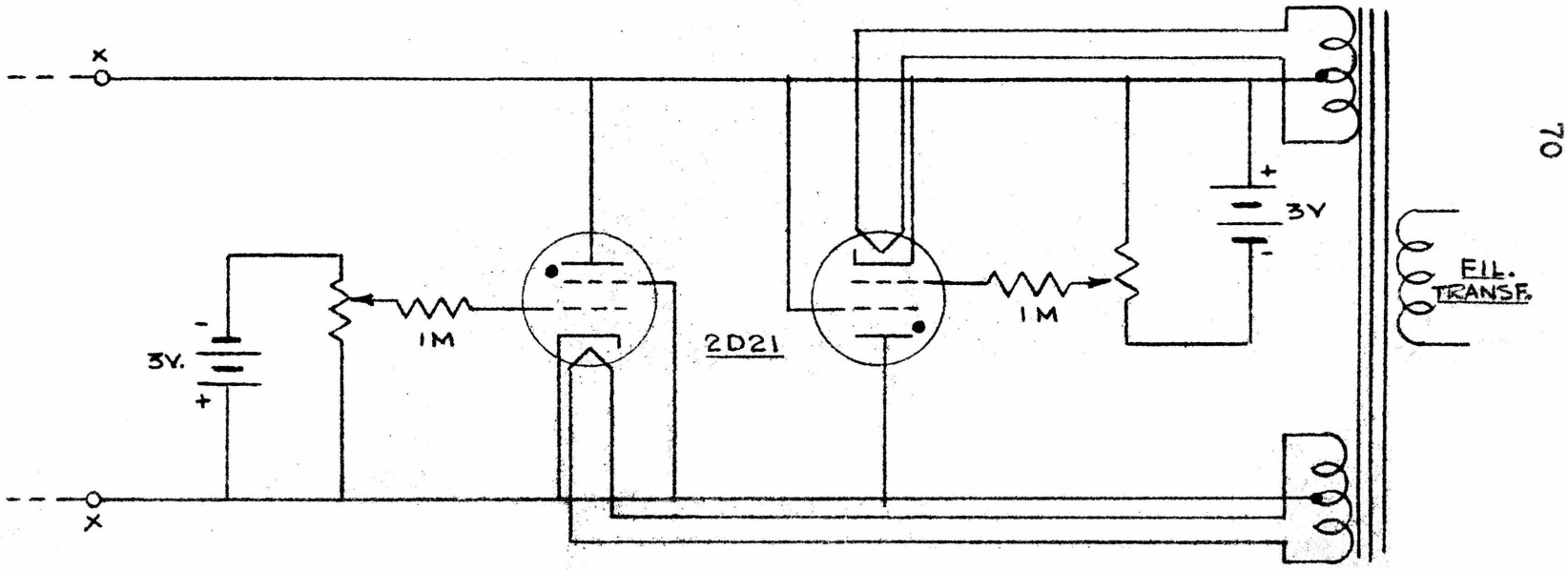

Fig. 4.8 THYRATRON ANALOG

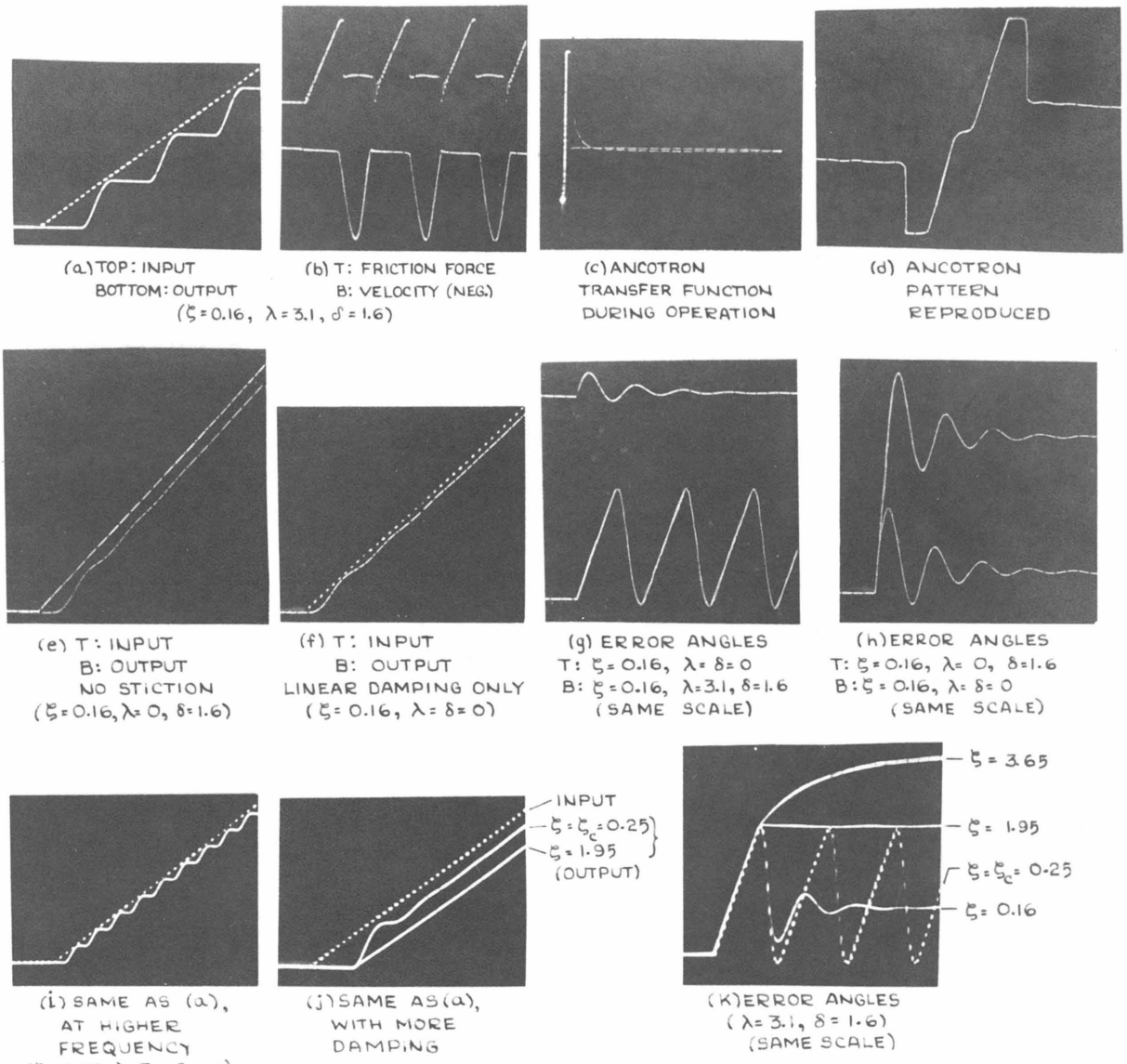

FIG. 4.9 CONSTANT VELOCITY INPUT

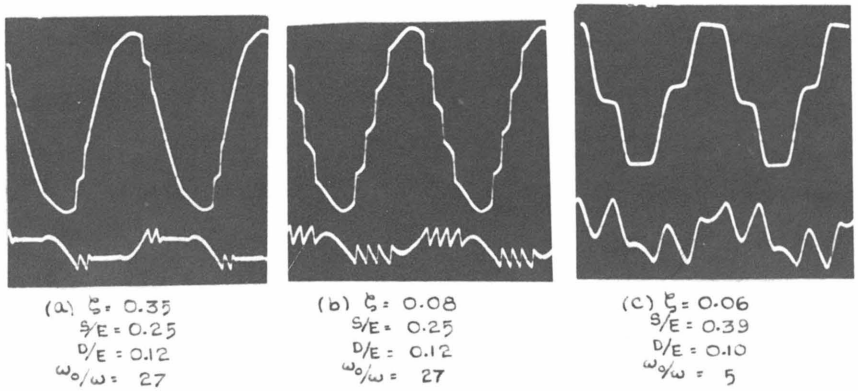

FIG. 4.10
SINUSOIDAL INPUT

TOP : OUTPUT ANGLE
BOTTOM: ERROR ANGLE

4.9 (a) shows the output or shaft angle (solid) and the input angle which is being followed. With a constant velocity the input angle increases linearly with time. Periodic chattering of the system, which has static and dynamic friction with but little viscous damping, is evident. First the servo sticks; then it suddenly breaks loose and tries to catch up with the input, but before it reaches the input angle the servo sticks again.

At the top of (b) is the output of the ancotron, that is, the friction torque, as a function of time, for the same system. At the bottom is the velocity (upside down) which is the input to the ancotron. The friction at first increases with the input angle and the velocity remains practically unchanged at zero; as it reaches the value S the friction suddenly drops to D and motion begins. As the velocity again reaches zero the system sticks, and friction takes over. The high-frequency transient oscillations are due to the ancotron but do not affect the solution.

(c) shows output (vertical) versus input (horizontal) of the ancotron during actual operation as in (b). The result closely approximates the assumed friction characteristic of Fig. 4.1, but only half the curve appears since the velocity does not change sign.

(d) is an oscillographic reproduction of the ancotron pattern with a linear sweep applied horizontally. The voltage limiters of Fig. 4.7 were removed to show the pattern itself.

The following pictures show the effect of various modifications. (e) is similar to (a) except that the static friction has been made equal to the dynamic friction ($\lambda = 0$). No chattering occurs. In (f) both static and dynamic friction have been reduced to zero so that only viscous friction remains. The steady-state error is seen to be less than for case (e).

The magnitude of the error angle (input minus output) for the different conditions is illustrated by (g) and (h). (g) compares the error for viscous friction alone (top) with that for all types of friction present (bottom); both records are to the same scale. (h) shows the error for viscous friction alone (bottom) compared to that with dynamic friction added (top) where static friction equals dynamic friction and hence no chattering takes place.

(i) shows chattering at a much higher frequency obtained by reducing the viscous damping; it demonstrates clearly that the phenomenon is periodic and does not decrease in magnitude.

(j) illustrates the effect of increasing the viscous damping for the system in (a). The top curve (dotted) is the input again, for reference. The next curve below it is obtained by increasing the damping to the point where the chattering has just disappeared. This is the critical case discussed in section 4. The change from periodic sticking in (a) to the highly damped oscillations shown here occurs suddenly, as predicted. If the viscous damping is increased further, the damped oscillations finally disappear entirely, giving the bottom curve. Note that ζ is about twice the value required to achieve this with linear damping alone.

Oscillogram (k) is a similar sequence for the error angle. The dotted line corresponds to (a). The solid curve at the bottom is the critical case where chattering has just stopped, and the next higher curve is the limiting case for which all oscillations have just been damped out; these two correspond to the output curves of (j). The curve at the top is for an overdamped system.

This last set of oscillograms of Fig. 4.9 demonstrates that any attempt to remove oscillations by

increasing the damping would result in larger steady-state errors. Damping should be kept just above the point where chattering sets in.

8. Sinusoidal Steady-State Input

If the servo is required to follow a motion which reverses periodically, the velocity will always go through zero. Some chattering is thus possible even when it does not occur for a constant input velocity. Photographic records are shown in Fig. 4.10 for a case where all three types of friction are present. In each picture the top curve is the output and the bottom curve the corresponding error angle.

In 4.10 (a) the linear damping is rather high and the chattering, which develops after the velocity has gone through zero, is damped out quickly. The damping is less for case (b) and chattering persists over the greater part of the sinewave to be followed.

Case (c), for which the input frequency has been made considerably higher relative to the natural frequency of the undamped system, shows excessive distortion due to the friction.

9. Step-Function Input

The response of a servo which is made to follow a sudden step change in the input angle is the same as if no stiction was present, provided the step is large enough so that the error causes a torque which exceeds the stiction. This case then reduces to that discussed in reference 22.

If the step is too small, the servo will remain at

rest. The minimum change in angle, of course, depends on the value of the static friction, and not the dynamic friction.

10. Thyratron Analog

After the investigation of the previous sections was completed, it was suggested that the rather complex ancotron circuit might be replaced by a pair of thyratrons.* Use is made of the fact that the voltage across the thyratron before firing (corresponding to the static friction S if the current corresponds to the velocity) is greater than the voltage after firing (corresponding to the dynamic friction D). By changing the grid bias the value of S can be changed over a wide range, but D is practically constant. No amplifiers are needed if the input voltage or current can be made large enough.

The thyratron circuit is given in Fig. 4.8. The bias on the tubes must be adjusted so that the values of S are equal. It may be necessary to match the tubes to obtain equal values of D. But if the input velocity does not change sign a single tube properly connected would suffice since the other tube would never conduct, anyway.

The circuit was tried and found to be satisfactory on the whole, except for some hash evident during the conducting period. This need not be serious.

---

* The writer is indebted to Peilin Luo for this suggestion.

APPENDIX A Critically Damped Linear Systems

Equation (2-3) with the forcing function of (2-4) becomes for a critically damped system ($\zeta = 1$)

$$\frac{d^2x}{d\tau^2} + 2\frac{dx}{d\tau} + x = 1 \qquad \text{(A-1)}$$

The solution for initial conditions of $x = \frac{dx}{d\tau} = 0$ is

$$x = 1 - (1 + \tau)e^{-\tau} \qquad \text{(A-2)}$$

Since this resembles an exponential curve, one might take the characteristic time of rise to be the value $\tau = 1$ in these dimensionless units. Then $x = 0.264$ at that point. For experimental work it is much easier and also more accurate to measure the time when $x = \frac{1}{2}$. This value will be denoted by τ_c and is given by the equation

$$(1 + \tau_c)e^{-\tau_c} = \frac{1}{2} \qquad \text{(A-3)}$$

By trial-and-error,

$$\tau_c = 1.68 \qquad \text{(A-4)}$$

APPENDIX B Underdamped Linear Systems with 10 % Overshoot

Equations (2-3) and (2-4), in general, combine to

$$\frac{d^2x}{d\tau^2} + 2\zeta\frac{dx}{d\tau} + x = 1 \qquad \text{(B-1)}$$

$$x = 1 - e^{-\zeta\tau}\left[\cos\left(\sqrt{1-\zeta^2}\,\tau\right) + \frac{\zeta}{\sqrt{1-\zeta^2}}\sin\left(\sqrt{1-\zeta^2}\,\tau\right)\right] \qquad \text{(B-2)}$$

The extremes of x occur when $\sqrt{1-\zeta^2}\,\tau = n\pi$ $(n = 0,1,2,\ldots)$ so that

$$\left.\begin{aligned} x_{max} &= 1 + e^{-n\pi\frac{\zeta}{\sqrt{1-\zeta^2}}} \qquad (n \text{ odd}) \\ x_{min} &= 1 - e^{-n\pi\frac{\zeta}{\sqrt{1-\zeta^2}}} \qquad (n \text{ even}) \end{aligned}\right\} \tag{B-3}$$

For a 10 % overshoot put $n = 1$ and

$$e^{-\pi\frac{\zeta_{10}}{\sqrt{1-\zeta_{10}^2}}} = 0.1000 \tag{B-4}$$

Hence

$$\zeta_{10} = \frac{1}{\sqrt{1 + \left(\frac{\pi}{\ln 10}\right)^2}} = 0.591155 \tag{B-5}$$

The time at which the first maximum is reached is

$$\tau_{10} = \frac{\pi}{\sqrt{1-\zeta_{10}^2}} = \sqrt{\pi^2 + (\ln 10)^2} = 3.895061 \tag{B-6}$$

APPENDIX C Critical Damping for Non-Linear Capacitance

Equation (2-13) together with (2-14), for positive x only, becomes

$$\frac{d^2x}{d\tau^2} + 2\zeta\frac{dx}{d\tau} + x^n = 1 \tag{C-1}$$

The solution for small ζ is known to approach $x = 1$ after some damped oscillations. In the region near $x = 1$ let $x = 1 - u$ and expand x^n by the binomial theorem. Neglecting higher terms, equation (C-1) becomes

$$\frac{d^2u}{d\tau^2} + 2\zeta\frac{du}{d\tau} + nu = 0 \tag{C-2}$$

This is a linear equation whose roots are $-\zeta \pm \sqrt{\zeta^2 - n}$. Hence (C-2) is critically damped if

$$\zeta_c = \sqrt{n} \tag{C-3}$$

Since the amount of damping is determined by the behavior of the system in the vicinity of $x = 1$ in general, the same condition should give critical damping

for equation (C-1) also.

APPENDIX D Derivation of Van der Pol's Equation for A Plate-Tuned Transformer-Coupled Oscillator

In the circuit shown in Fig. 3.1 the coil losses are represented by a parallel conductance G .* L is the self-inductance of the plate coil. Grid current is neglected.

The plate current i_p is a function both of the grid voltage v_g and the plate voltage v. But these are related by

$$v_g = -\frac{M}{L} v \qquad \text{(D-1)}$$

the sign being that required to obtain oscillations. Therefore one can write

$$i_p = \psi(v) \; . \qquad \text{(D-2)}$$

Circuit equation:

$$i_p = -G v - C \dot{v} - \frac{1}{L}\int v \, dt \qquad \text{(D-3)}$$

or

$$\ddot{v} + \frac{G}{C}\dot{v} + \frac{1}{C}\frac{d}{dt}\left[\psi(v)\right] + \frac{1}{LC} v = 0 \qquad \text{(D-4)}$$

Let $\omega_o = 1/\sqrt{LC}$, $Q = \omega_o C/G$, $\tau = \omega_o t$.

Let v_o be a characteristic value of v, such as the "Saturation" plate voltage. Then

$$\frac{d^2}{d\tau^2}\left(\frac{v}{v_o}\right) + \frac{d}{d\tau}\left[\frac{1}{Q}\frac{v}{v_o} + \varphi\left(\frac{v}{v_o}\right)\right] + \frac{v}{v_o} = 0 \qquad \text{(D-5)}$$

where $\varphi\left(\frac{v}{v_o}\right) = \frac{1}{v_o}\sqrt{\frac{L}{C}}\,\psi(v)$.

Expanding $\varphi(v/v_o)$ in a power series up to the

---

* Van der Pol and other writers use a resistance in series with the coil which puts another term into the equations. To obtain the desired result this term must eventually be neglected. The parallel circuit gives the answer directly. Furthermore, with iron-core coils, it is doubtful whether a series resistance represents the losses over a range of frequencies any more accurately than a parallel one.

third-order term gives

$$\varphi\left(\frac{v}{v_o}\right) = - \alpha \frac{v}{v_o} + \gamma \left(\frac{v}{v_o}\right)^3 + \ldots \qquad \text{(D-6)}$$

The linear term will be negative since, from linear circuit theory,

$$i_p = g_m v_g + g_p v = - \left(g_m \frac{M}{L} - g_p\right) v \qquad \text{(D-7)}$$

Even-order terms can be neglected by assuming symmetry about the operating point. Then, putting $\mu = \alpha - 1/Q$ and $u = \sqrt{\frac{3\gamma}{\mu}} \frac{v}{v_o}$, equation (D-5) is transformed into Van der Pol's equation (3-3).

Van der Pol[13] showed also that if $\varphi(v/v_o)$ is expanded up to the fifth-order term, and if the third-order term is negative, but the linear and fifth-order terms are positive, the system has the characteristics of "hard excitation" (page 58).

APPENDIX E Derivation of Van der Pol's Equation for A Symmetrical Multivibrator

The analysis follows Van der Pol's[14] in the main features, except for the use of the stray grid-cathode capacitance C_g instead of the lead inductance L used by him. The effect of C_g would overshadow any effect due to L at the frequencies used. See Fig. 3.2.

Node equations for the circuit:

$$g\, v_{g1} + (C + C_g)\, \dot{v}_{g1} - C\, \dot{v}_{p2} + i_{g1} = 0 \qquad \text{(E-1)}$$

$$i_{p2} + G\, v_{p2} + C\, \dot{v}_{p2} - C\, \dot{v}_{g1} = 0 \qquad \text{(E-2)}$$

Similarly for the other two nodes.

Now assume that $C\,(\dot{v}_p - \dot{v}_g) \ll i_p$ and $i_g \ll i_p$. Then with symmetrical tubes the plate currents possess approximately symmetrical half-cycles, so that

$$i_{p1} \approx - i_{p2} \qquad \text{(E-3)}$$

The tubes alternately saturate (grid current flows)

and cut off (no grid current). The tube which draws grid current discharges its condenser quite rapidly. But nothing more happens until the other tube is ready; its condenser discharges with the large time constant C/g as no grid current flows. Thus the tube which is cut off always determines the start of the next transition. The grid current, even though it may be quite large momentarily, does not affect the overall circuit behavior, and hence one can put $i_g = 0$ in the circuit equations.

Equation (E-2) thus becomes

$$- i_{p2} = i_{p1} = G\, v_{p2} + C\,(\dot{v}_{p2} - \dot{v}_{g1}) \qquad \text{(E-4)}$$

Combining with equation (E-1) gives

$$\frac{C_g}{g}\frac{C}{G}\ddot{v}_{g1} + \left(\frac{C + C_g}{g} + \frac{C}{G}\right)\dot{v}_{g1} + v_{g1} - \frac{C}{gG}\dot{i}_{p1} = 0 \qquad \text{(E-5)}$$

Now let

$$\tau = \sqrt{\frac{g}{C_g}\frac{G}{C}}\, t$$

$$\sqrt{\frac{C}{C_g}}\frac{1}{\sqrt{gG}}\, i_{p1} \approx \left[-\alpha\frac{v_{g1}}{v_o} + \left(\frac{v_{g1}}{v_o}\right)^3\right] v_o$$

$$\mu = \alpha - \left(\sqrt{\frac{C}{C_g}\frac{G}{g}} + \sqrt{\frac{C}{C_g}\frac{g}{G}} + \sqrt{\frac{C_g}{C}\frac{G}{g}}\right)$$

$$\text{and} \quad u = \sqrt{\frac{3\gamma}{\mu}}\frac{v_{g1}}{v_o}$$

where v_o is the reference value of v_{g1}. Then equation (C-5) transforms into Van der Pol's equation (3-3).

Note that the variable u now stands for the grid-cathode voltage of one of the tubes. To the extent that the plate current expansion represents the tube characteristics, the solution of Van der Pol's equation will give the frequency of the oscillation quite accurately. The waveform will not be that of the grid-cathode voltage, since grid current makes it decidedly unsymmetrical. However, if the grid-cathode voltage of each tube can be assumed to be essentially zero during the conducting half-cycle, the variable u does give the grid-to-grid voltage waveform.

APPENDIX F

ANCOTRON – CIRCUIT DIAGRAM

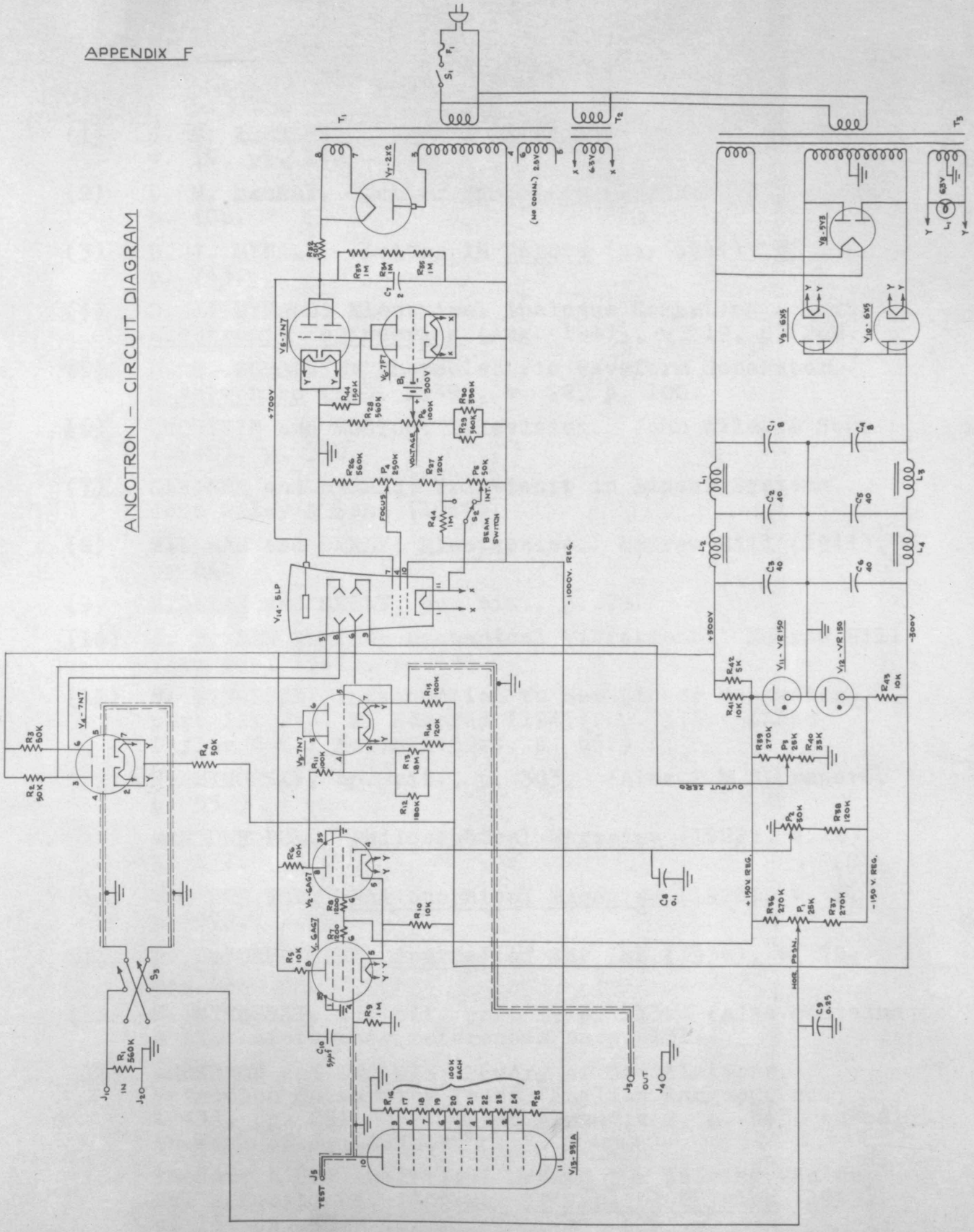

REFERENCES

(1) J. S. KOEHLER. Journal of Applied Physics (1948), v. 19, pp. 148 - 155.

(2) D. M. MacKAY. Letter in Nature (March 1947), v. 159, p. 406.

(3) D. J. MYNALL. Letter in Nature (May 1947), v. 159, p. 743.

(4) D. J. MYNALL: Electrical Analogue Computing - Part 3. Electronic Engineering (Aug. 1947), v. 19, p. 262.

(5) D. E. SUNSTEIN: Photoelectric Waveform Generator. Electronics (Feb. 1949), v. 22, p. 100.

(6) ZWORYKIN and MORTON: Television. John Wiley & Sons (1940), p. 350.

(7) GARDNER and BARNES: Transients in Linear Systems. John Wiley & Sons (1942).

(8) MILLMAN and SEELY: Electronics. McGraw-Hill (1941), p. 64.

(9) MILLMAN and SEELY, op. cit., p. 79.

(10) J. P. DEN HARTOG: Mechanical Vibrations. McGraw-Hill (3rd ed., 1947), p. 433.

(11) N. MINORSKY: Introduction to Non-Linear Mechanics, part III. J. W. Edwards (1947), p. 313. (Also Taylor Model Basin report, p. 65.)

(12) N. MINORSKY, op. cit., p. 303. (Also T.M.B. report, p. 55.)

(13) VAN DER POL. Philosophical Magazine (1922), v. 43, p. 177.

(14) VAN DER POL. Philosophical Magazine (1926), v. 2, p. 978.

(15) P. LeCORBEILLER. Journal of the IEE (1936), v. 79, p. 361.

(16) N. MINORSKY, op. cit. part I, p. 113. (Also contains a list of further references on p. 131.)

(17) ANDRONOW and CHAIKIN: Theory of Oscillations. Princeton University Press (English language ed., 1949), pp. 251, 252. Also Appendix C, p. 343, based on work of J. LASALLE.

(18) SHOHAT: A New Analytical Method for Solving Van der Pol's Equations. Journal of Applied Physics (1943), v. 14, pp. 40 - 48.

(19) DEN HARTOG, op. cit., p. 439.

(20) DEN HARTOG, op. cit., p. 435.

(21) S. TIMOSHENKO: Vibration Problems in Engineering. D. Van Nostrand (2nd ed., 1937), pp. 30 and 54.

(22) G. D. McCANN, F. C. LINDVALL, and C. H. WILTS: The Effect of Coulomb Friction on the Performance of Servomechanisms. Transactions of the AIEE (1948), paper 48-84.

(23) DEN HARTOG, op. cit., p. 354.

(24) Massachusetts Institute of Technology Radiation Lab. Series, vol. 21: Electronic Instruments. McGraw-Hill (1948), p. 357.

(25) EYRES, HOWLETT, MICHEL, and PORTER: A Theoretical Investigation of the Effects of Stiction and Coulomb Friction on the Minimum Smooth Running Speed of a Metadyne Controlled Motor... Air Defence Research and Development Establishment (British), Report no. 180. (Numerical results given in that report agree in general, but not too closely, with those of part IV.)

Papers describing the Caltech Electric Analog Computer:

(26) E. L. HARDER and G. D. McCANN: A Large-Scale General-Purpose Electric-Analog Computer. Transactions of the AIEE (1948), paper 48-112.

(27) G. D. McCANN, C. H. WILTS, and B. N. LOCANTHI: Electronic Techniques Applied to Analog Methods of Computation. Presented at 1948 IRE Pacific Coast Convention; to be published in the Proceedings of the IRE.

(28) G. D. McCANN, C. H. WILTS, and B. N. LOCANTHI: Application of the CalTech Electric Analog Computer to Nonlinear Mechanics and Servomechanisms. Transactions of the AIEE (1949), paper 49-165.